INVESTIGATION OF Ni-Mo/SBA-15 AS HYDROTREATING CATALYST – COMPARISON WITH Ni-Mo/Al$_2$O$_3$

A project report

submitted in partial fulfillment of the requirements

for the award of the degree of

MASTER OF TECHNOLOGY

in

CATALYSIS TECHNOLOGY

by

ADITYA V. AJGAONKAR

(CA10M001)

Under the guidance of

PROFESSOR S. PUSHPAVANAM

Dr. S. SIVASANKER

DEPARTMENT OF CHEMICAL ENGINEERING

INDIAN INSTITUTE OF TECHNOLOGY- MADRAS

CHENNAI 600 036

MAY 2011

CERTIFICATE

This is to certify that the thesis entitled "**INVESTIGATION OF Ni-Mo/SBA-15 AS HYDROTREATING CATALYST – COMPARISON WITH Ni-Mo/Al$_2$O$_3$**", submitted by **Mr. ADITYA V. AJGAONKAR (CA10M001)** to the Indian Institute of Technology-Madras, Chennai for the award of the degree of Master of Technology in Catalysis Technology (Chemical Engineering), is a *bona-fide* record of the work carried out by her under our supervision. The contents of this thesis, in full or in parts, have not been submitted to any other Institute or University for the award of any degree.

Guide   **Co Guide**

Dr. S. PUSHPAVANAM   Dr .S.SIVASANKER

Department of Chemical Engineering   National Centre for Catalysis Research

IIT – Madras   IIT Madras

Chennai – 600 036   Chennai – 600 036

Place : Chennai

Date : May 01 , 2011

ACKNOWLEDGEMENTS

ABSTRACT

In petroleum refinery, crude oil is distilled into several fractions like naphtha, gas oil etc. after the pretreatment. Due to strict environmental regulations, the use of "Clean Fuels" is now necessary. Furthermore, most of the catalysts which are used in refinery processes are not tolerant to sulfur, nitrogen and metals. In addition, due to shift in the feedstock towards the heavier fractions such as atmospheric and vacuum residue in which most of the sulfur, nitrogen and metal compounds are present, removal of these impurities is very important. Hydrotreating is the process by which the feedstock is reacted with hydrogen at high pressures and moderate to high temperatures for the removal of sulfur, nitrogen and metal compounds. Catalysts used in the industry for carrying out hydrotreating are generally cobalt or nickel – molybdenum supported on gamma alumina.

Over the years, considerable efforts have been made to study the properties of alumina supported, sulfided cobalt – molybdenum, nickel –molybdenum catalysts. This has included efforts to identify the active sites, the role of promoters, influence of preparation and activation conditions etc. Due to its outstanding textural and mechanical properties, alumina has been used exclusively. Another important factor is the ability to regenerate catalytic activity after intensive use in the hydrotreating reactions.

In order to improve the activity of hydrotreating catalysts and to reduce the severity of experimental conditions, several approaches have been pursued. One such approach is to improve the support for the active components. With the advent of mesoporous materials, catalysts like MCM-41 have been studied extensively.

In order to understand the mechanism of the reactions and laboratory testing of the catalysts, several model compounds have been used.

In this work Ni-Mo supported on gamma-alumina and SBA-15 were prepared in the laboratory and used. The catalysts were characterized using x-ray powder diffraction (XRD), temperature programmed desorption (TPD), temperature programmed reduction (TPR), transmission electron microscopy (TEM) and BET Surface area determination methods.

Three types of the hydrotreating reactions, hydrodenitrogenation (HDN), hydrodesulfurization (HDS) and hydrodemetallation (HDM) to remove nitrogen, sulfur and metals, respectively were carried out under industrial hydrotreating -conditions using a fixed bed microreactor and sulfide forms of the catalysts (Ni-Mo/Al$_2$O$_3$ and Ni-Mo/SBA-15). Quinoline (Q) and tetrahydroquinoline (1-THQ) were used as model compounds for HDN studies, dibenzothiophene (DBT) and 4,6-dimethyl dibenzothiophene (DMDBT) were used as model compounds for the HDS reaction and Ni-tetraphenylporphyrin was used to investigate the HDN reaction. Reaction parameters such as temperature and contact time have been studied to evaluate the nature of the active sites and the reaction mechanism. Studies on simultaneous hydrodesulphurization (HDS) of DBT and 4,6-DMDBT was also investigated over the catalysts and the reaction pathway was identified for DBT and DMDBT.Hydrodemetallation of nickel tetraphenylporphyrin (Ni-TPP) was carried out over both the catalysts. The conversion of the nickel porphyrins was estimated using UV-Vis absorbance studies. A relative evaluation of the three hydrotreating reactions over the two catalysts is presented.

TABLE OF CONTENTS

List of Tables

List of Figures

Abbreviations

LPG	Liquified petroleum gas
ppm	Parts per million
g	grams
psi	Pounds per square inch
VGO	Vacuum gas oil
CCR	Conradson carbon residue
HDT	Hydrotreating
HDS	Hydrodesulfurization
HDN	Hydrodenitrogenation
HDM	Hydrodemetallation
SBA-15	Santa Barbara amorphous type material
XRD	X-ray powder diffraction
BET	Brunnauer, Emmet and Teller
TPD	Temperature programmed desorption
TPR	Temperature programmed reduction
UV-Vis	Ultraviolet visible spectroscopy
TEM	Transmission electron microscopy
Q	Quinoline
1-THQ	1,2,3,4-tetrahydroquinoline
DBT	Dibenzothiophene
4,6-DMDBT	4,6-dimethyl dibenzothiophene
API	Americal petroleum institute
DHQ	Decahydroquinoline
5-THQ	5,6,7,8-tetrahydroquinoline
OPA	o-propyl aniline
PCHE	Propyl cyclohexene
PCHA	Propyl cyclohexyl amine
PCH	Propyl cyclohexane
PB	Propyl benzene
Ni	Nickel

Mo	Molybdenum
V	vanadium
W	Tungsten
Co	cobalt
Ir	Iridium
Os	Osmium
Pd	Palladium
Pt	Platinum
Ru	Ruthenium
Rh	Rhodium
Ti	Titanium
Al_2O_3	Alumina
DDS	Direct desulfurization
HYD	Hydrogenation
H_2S	Hydrogen sulfide
APD	Average pore diameter
Ni-TPP	Nickel tetraphenylporphyrin
nm	Nanometer
MW	Molecular weight
He	Helium
HPLC	High pressure liquid chromatography
GC	Gas Chromatography
WHSV	Weight hourly space velocity
GC-MS	Gas chromatography mass spectroscopy
MoS_2	Molybdenum sulfide
NiS	Nickel Sulfide
S_{BET}	Surface areas calculated by the BET method
S_{Ext}	Area obtained after subtracting t-plot micropore area from S_{BET}
PV_{total}	Total pore volume
PV_{meso}	Mesopore volume
MoO_3	Molybdenum oxide
Cu Cr	Cumene Cracking

BP   Biphenyl

CHB   Cyclohexylbenzene

BCH   Bicyclohexyl

MCH   Methyl cyclohexane

MCHT   Methyl cyclohexyl toluene

DMBP   Dimethyl biphenyl

NOTATIONS

wt%	Weight %
C	Carbon
^{0}F	Degree fahrenheit
^{0}C	Degree celsius
γ	Gamma (Type of alumina)
α	Alpha (Type of alumina)
η	Eta (Type of alumina)
δ	Delta (Type of alumina)
θ	Theta (Type of alumina)
K	Kelvin
λ	Lambda (wavelength)
T_d	Tetrahedral co-ordination
O_h	Octahedral co-ordination

CHAPTER I

INTRODUCTION

1.1 GENERAL INTRODUCTION

Petroleum refining is the separation of crude petroleum oil into fractions and the subsequent treating of these fractions to yield marketable products. The main goal in oil refining is to provide the marketplace with the required quantities and qualities of products such as fuels [liquefied petroleum gas (LPG), gasoline, kerosene, diesel oil, heating oil and heavy fuels] and specialties (such as solvents, lube oils) and also chemical intermediates (like olefins and aromatics). Today the major feedstock used in petroleum refining is crude oil with some condensates obtained from gas fields [Speight , 2007].

Crude oil is a complex liquid mixture made up of a vast number of hydrocarbon compounds and is characterized by their high carbon and hydrogen contents. Crude oils are composed of thousands of individual compounds: paraffins, cycloalkanes and aromatics with molecular weights up to several thousand g mol^{-1}. In addition, small amounts of organic compounds containing sulfur, nitrogen, oxygen and metals such as vanadium, nickel, iron and copper are present. The content of heteroatoms is in the range from 0.1 to a few weight % (wt %). The content of the metals varies from few ppm up to 1000 ppm depending upon the source of the crude oil. Apart from these heteroatoms and metal containing compounds very small quantities of phosphorus, arsenic and mercury may also be found at ppm levels [Speight, 2007].

To convert crude oil into desired products in an economically feasible and environmentallyacceptable manner, refinery process for crude oil are generally divided into three categories:

1. *Separation processes* such as distillation, solventdeasphalting, solvent extraction, and solvent dewaxing.
2. *Conversion processes* such as coking, reforming, catalytic cracking etc.
3. *Finishing processes* such as hydrotreating.

1.1.1 Key Catalytic processes in Petroleum Refining:

1.1.1.1 Catalytic Reforming:

Reforming represents the total effect of numerous reactions such as cracking, polymerization, dehydrogenation and isomerization taking place simultaneously.In this process a special catalyst (platinum supported on alumina) is used to restructure naphtha fraction (C_6-C_{10}) into aromatics and isoparaffins. The produced naphtha reformate has a much higher octane number than the feed. This reformate is used in gasoline formulation and as a feedstock for aromatic production [Faheem, 2010].

1.1.1.2 Catalytic Cracking:

Catalytic cracking breaks complex hydrocarbons into simpler molecules in order to increase the quality and quantity of lighter, more desirable products and decrease the amount of residuals. This process rearranges the molecular structure of hydrocarbon compounds to convert heavy hydrocarbon feedstock into lighter fractions such as kerosene, gasoline, LPG, heating oil and petrochemical feedstock.Catalytic cracking is similar to thermal cracking except that catalysts facilitate the conversion of the heavier molecules into lighter products. Use of a catalyst in the cracking reaction increases the yield of improved-quality products under much less severe operating conditions than in thermal cracking. Typical temperatures range from 850°-950° F at much lower pressures of 10-20 psi.

Clay, amorphous silica alumina and zeolites are the constituents of catalytic cracking catalysts[Faheem, 2010].

1.1.1.3 Isomerization:

Isomerization of light naphtha is the process in which low octane numberhydrocarbons (n-C_5, n-C_6) are transformed into branched products with thesame carbon number. This process produces high octane number products.Generally naphtha is hydrotreated and fractionated into light and heavy naphthaboiling below 80 °C and between 90– 190°C (190–380 deg F). The heavier fraction is used as a feed to the reforming unit and the lighter fraction is sent to the isomerization unit. Light hydrocarbons tend to hydrocrack in

the reformer and C_6 hydrocarbons tend to form benzene in the reformer. Gasoline specifications require very low value of benzene due to carcinogenic effect.

For isomerization reaction,monofunctional acidic as well as bifunctional acidic catalysts can be used. Monofunctional catalysts deactivate faster with time on stream. Bifunctional acidic catalysts such as Pt supported on chlorinated alumina with high chlorine content, zeolites and sulfated zirconia are typical catalysts. Bifunctional acidic catalysts possess stable isomerization activity at high hydrogen pressures (10 – 30 bars)[Faheem, 2010].

1.1.1.4 Alkylation:

Alkylation is the process of producing gasoline range material (alkylates)from olefins such as propylene ($C_3^=$), butylenes ($C_4^=$) and amylene($C_5^=$), and isobutane. Butylene is the most widely used olefin because of thehigh quality of the alkylate produced. The current trend towards eliminationof methyl tertiary butyl ether (MTBE) has resulted in increased attention toalkylation technology. In industry alkylation reaction is catalyzed by liquid HF and H_2SO_4[Faheem, 2010].

Various solid acid catalysts such as acid forms of zeolites, liquid Bronsted or Lewis acids coated on solid supports, sulfated zirconia / titania, chlorinated alumina modified with alkali metals have also been investigated. However short time on stream and shift in selectivity towards oligomerization of alkenes were found to be the main disadvantages [Weitkamp, 2008].

1.1.1.5 Catalytic Hydrocracking:

Hydrocracking is a two-stage process combining catalytic cracking and hydrogenation, wherein, heavier feedstocks are cracked in the presence of hydrogen to produce more desirable products. The process is carried out in fixed bed reactor in which liquid oil feedstock and gaseous hydrogen are passed in a down-flow mode over catalyst beds at pressures ranging from 80-200 bars and temperatures ranging from 300-450 °C. The first stage involves primarily feedstock pretreatment in which heterocyclic organic compounds such as those containing sulfur, nitrogen and oxygen are converted into hydrocarbons.

3

Further, hydrogenation of aromatic hydrocarbons also takes place to an appreciable extent. In the second stage, cracking takes place. The conversion levels in the second stage are limited to 30-70 % per pass to obtain desiredselectivities; this necessitates the recycle of unconverted oil in the second stage for achieving total conversions close to 100%.

In the first stage, catalysts based on Ni-Mo and Ni-W are used based on the nitrogen level in the feed and the desired hydrogenation of feed compounds. In cases where concentrations of sulfur are low, a metal such as Pd may be used as the hydrogenation function. Such Pd based catalysts are found to be more active in hydrogenation reactions compared to mixed sulfide containing catalysts. For cracking function, acidic supports such as alumina, fluorinated alumina, amorphous silica-alumina and zeolites are used. Zeolites provide in general the highest cracking activity; however they may suffer from mass transfer limitations leading to lower product selectivities[Rob Van Veen , 2008].

1.1.1.6 Hydrotreating:

The major use of supported metal sulfides is in the removal of sulfur, nitrogen, oxygen and metals from oil fractions by reductive treatments in so-called hydrotreating processes. Hydrotreating is the key process used widely in the refineries for achieving the following objectives:

1. Removing impurities mentioned above for the control of the final product specification or for the preparation of feed for the further processing (naphtha reformer feed and FCC feed).
2. Removal of metals, usually in a separate guard catalytic reactor where the organo-metallic compounds are hydrogenated and decomposed, resulting in the metal deposition in the catalyst pores (atmospheric residue desulfurization (ARDS) guard reactor)
3. Saturation of olefins and their unstable compounds.

The various hydrotreating processes based on the feedstocks used and products obtained are listed below in Table 1.1[Faheem, 2010].

4

Feedstock	Products	Type of process	Impurities Removal
Naphtha	Reformer Feed	Hydrotreating	Sulfur
Atmospheric gas oil	Diesel	Hydrotreating	Sulfur, Aromatics
	Jet Fuel	Mild Hydrocracking	Sulfur, Aromatics
Vacuum Gas Oil (VGO)	Low sulfur fuel oil (LFSO)	Hydrotreating	Sulfur
	FCC Feed	Hydrotreating	Sulfur, Nitrogen and Metals
	Diesel	Hydrotreating	Sulfur , Aromatics
	Kerosene / Jet fuel	Hydrotreating	Sulfur, Aromatics
	Naphtha	Hydrotreating	Sulfur, Aromatics
	Lube Oil	Hydrotreating	Sulfur, Nitrogen and aromatics
Residuum	LSFO	Hydrotreating	Sulfur
	FCC Feedstock	Hydrotreating	Sulfur, Nitrogen, Metals and CCR
	Coker Feedstock	Hydrotreating	Sulfur, Nitrogen, Metals and CCR

Table 1.1 Different hydrotreating processes based on feedstock and products

Many new challenges continue to arise in the field of hydrotreating. There is a dramatic decrease in the demand of fuel oil worldwide resulting in need for the conversion of heavier fractions into light distillates for transportation use. Other challenges in hydrotreatingresult from the environmental legislations which place increasingly severe restrictions on gaseous and particulate emissions arising both from the refinery and the use of heating and transportation fuels. Although there are significant variations from region to region, it is clear that environmental regulations will pose the major driving force for the introduction of more hydrotreating in refineries.

Hydrotreating is the generic name given to processes utilizing hydrogen, which include processes like hydrodesulphurization (HDS), hydrodenitrogenation (HDN), hydrodeoxygenation (HDO), hydrodechlorination (HDCl) and hydrodemetallation (HDM) used for removal of sulfur, nitrogen, oxygen, chlorine, metals from heteroatomic compounds present in the crude oil or products respectively. Out of the processes listed above HDS, HDN are widely used for treating crude oil and to produce a wide range of feedstocks as well as products to meet environmental specifications, while HDM is used to remove metals from heavy (high boiling) feeds such as residuum to avoid the detrimental effect of these metals on

catalysts used in downstream processing, discussed in later chapter. Thus hydrotreating catalysts constitute the third largest business in catalysts after exhaust gas catalysts and cracking catalysts [Prins, 2008].

1.2   RESEARCH OBJECTIVES

The objective of this work is to study the utility of SBA-15, an ordered mesoporous SiO_2 as a support for Ni-Mo catalysts used in hydrotreating reactions. It is proposed to compare the performance of NiO and MoO_3 supported on SBA-15 (Ni-Mo/SBA-15) as a hydrotreating catalystwith conventional Ni-Mo/Al_2O_3. The specific hydrotreating reactions to be investigated are hydrodenitrogenation (HDN), hydrodesulphurization (HDS) and hydrodemetallation (HDM). Model compounds, viz. quinoline and 1,2,3,4-tetrhydroquinoline will be used to investigate the HDN reaction, while dibenzothiophene and 4,6-dimethyldibenzothiophene will be used to investigate the HDS reaction. Ni-tertraphenylporphyrin will be used to study hydrodemetallation. The reaction pathways followed over the two catalysts has been evaluated using different reaction parameters such as temperature and contact time. The supports and catalysts are to be characterized by many physic-chemical methods to identify the nature of the active species present in the catalysts. The characterization results will be utilized to understand the relative performance of the two catalysts.

1.3   SCOPE OF THE THESIS AND ORGANIZATION OF CHAPTERS

The thesis has been divided into six chapters and the outline of the chapters is given below;

Chapter 1 has comprised of a general introduction for hydrotreating reactions and their importance. The scope and objectives of the present investigation have been outlined at the end of this chapter.

Chapter 2 involves a literature survey of hydrotreating reactions, especially, HDN, HDS and HDM and the catalysts used in these reactions.

Chapter 3lists the chemicals used, explains the different procedures for the preparation of the catalysts and describes instrumental methods used for analyzing the physico-chemical characteristics of the catalysts and supports. A description of the high pressure reactor used,

the procedures adopted for carrying out the reactions and the analytical methodologies adopted for evaluating catalyst performances are also presented.

Chapter 4. This chapter consists of two parts.

Part 1 discusses the results of the characterization of the supports and catalysts using XRD, N_2-adsorption, TPD, TPR, UV-Vis., TEM, Raman techniques.

Part 2 focuses on the hydrotreating recations such as hydrodenitrogenation, hydrodesulphurization and hydrodemetallation carried out over sulfided Ni-Mo/SBA-15 and Ni-Mo/Al$_2$O$_3$ catalysts.

Chapter 5 summarizes the results obtained on characterization of the catalysts and the reactions at the end of this chapter.

CHAPTER II
LITERATURE SURVEY

2.1 HETEROCYCLIC COMPOUNDS IN PETROLEUM

2.1.1 Nitrogen compounds in Petroleum

The type of N-compounds and the total amount of nitrogen vary from feed to feed. The type of nitrogen compounds present in the crude oil are shown in Table 2.1. Polycyclic aromatic nitrogen compounds, such as quinoline, indole, acridine and carbazole are the main nitrogen containing compounds in oil products, while monocyclic pyridine, pyrrole and anilines and their derivatives are present in coal tar.
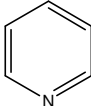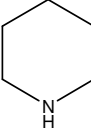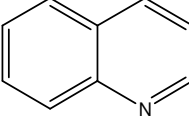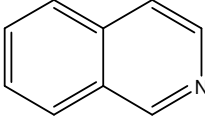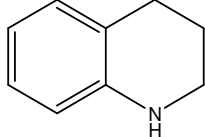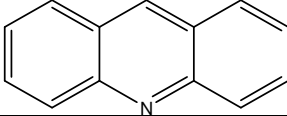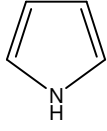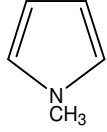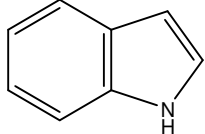
Polycyclic nitrogen containing compounds can be divided into five membered and six-membered N-ring compounds, classified as non-basic and basic N-compounds, respectively. In non-basic nitrogen compounds, pyrroles are five-membered heteroaromatic compounds containing one nitrogen atom. When fused with the benzene ring, pyrrole is converted into the polycyclic heteroaromatic compounds,indole and carbazole.Pyridines are six-membered heteroaromatic compounds containing onenitrogen atom. When fused with benzene rings, pyridines are converted intothe polycyclic heteroaromatic compounds quinolines and isoquinolines.

Anilines account for only small portion of nitrogen in conventional feeds: however, their content in synthetic crudes produced through coking or catalytic cracking can be much higher [Prins ,1997].

Kasztelan *et al.,*1991 provided a breakdown of the nitrogen content in distillation cuts obtained from several sources. As shown in Table 2.2,nitrogen content is morein the heavier fractions of the feed. There is also diversity in the distribution of the nitrogen compounds. The composition of the middle distillate fractions derived from oil shale, tar sands, and conventional petroleum and published by Mushrush *et al.* are shown in Table 2.3. The middle distillates were hydrotreated prior to analysis. The total nitrogen content in the distillates, obtained from shale oil and tar-sands was found to be very high compared to petroleum based

middle distillates. Several types of nitrogen compounds discussed above were found to be present in different proportions.

Table 2.1: Typical nitrogen compounds found in crude oil

Compound	Structure
Six Membered Heterocyclic	
Pyridine (PY)	
Piperidine (PIP)	
Quinoline (Q)	
Iso-quinoline (IQ)	
Tetrahydroquinoline (THQ)	
Acridine (ACR)	
Five Membered Heterocyclic	
Pyrrole (PYR)	
Methyl Pyrrole (MePyr)	
Indole (IN)	
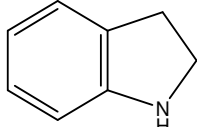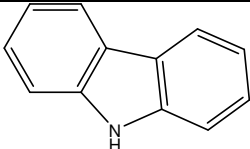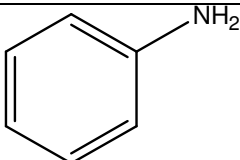
Indoline (IND)	
Cabazole (CAR)	
Non Heterocyclic	
Aniline (ANI)	

Table 2.2: Typical N contents of straight run and conversion processsproducts (Kasztelan *et al.,*1991)

Feed	Cut	Nitrogen (ppm)
Straight run	Naphtha	2
Arabian light	Gas oil	430
	Vacuum gas Oil	1200
FCC products from vacuum gas oil	Gasoline	23
	Gas oil	600
	Heavy gas oil	2100
Delayed coking	Gasoline	165
	Gas oil	630
Fluid coking	Heavy gas oil	8000
Visbreaking	Gasoline	15
	Gas oil	500
	Vacuum oil	2600

Table 2.3: Distribution of N-compounds (%) in middle distillates (Mushrush *et al,* 1999)
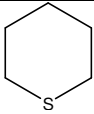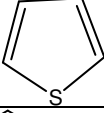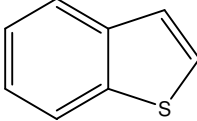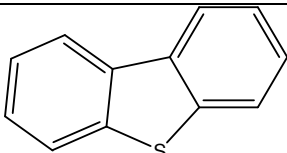
Feed	Shale	Petroleum	Tar-sands
Total N, ppm	2290	83	3050
Boiling Range, deg C	150-390	220-384	190–390
CARs	1.3	0.5	3.2
INs	3.7	18.1	39.2
PYs	73.5	64.3	13.3
PYRs	3.6	0.2	15.9
Qs	4.3	10.4	1.2
THQs	9.9	3.2	16.7
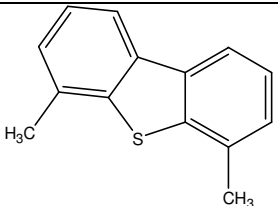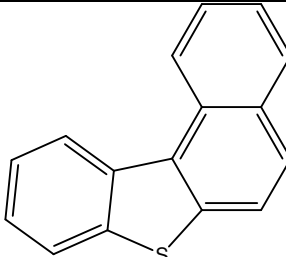
2.1.2 Sulfur compounds in Petroleum

Organosulfur compounds are present in almost all crude oil fractions. The sulfur content of petroleum varies from less than 0.05 to more than 14 % wt., but generally falls in the range 1 to 4 % wt. Crude oil contains sulfur heteroatoms in the form of elemental sulfur S, dissolved hydrogen sulfide H_2S, carbonyl sulfide COS, inorganic forms and most importantly organic forms.

The low boiling crude oil fraction contains mainly aliphatic organosulfur compounds viz. thiols, sulfides and disulfides. They are very reactive and can be easily removed. The higher boiling fractions, such as heavy straight-run naphtha, straight run diesel, and fluid catalytic cracking (FCC) naphtha, contain thiophenes, benzothiophenes, and their alkylated derivatives. Different sulfur compounds present in crude oil are shown in Table 2.5

Table 2.5: Typical sulfur compounds found in crude oil

Compound	Structure
Thiols (mercaptans)	RSH
Sulfides	RSR'
Disulfides	RSSR'
Cyclic sulfides	
Thiophene (TH)	
Benzothiophene (BT)	
Dibenzothiophene (DBT)	

4,6-dimethyldibenzothiophene (4,6-DMDBT)	
Naphthobenzothiophene	

In general, higher the density of the crude oil, lower the API gravity of the crude oil and higher the sulfur content. Although it has been cited that the proportion of the sulfur compounds increases with boiling point during distillation [Speight, 2000], the middle fraction may actually contain more sulfur than higher boiling fractions as a result of the break-down of higher molecular weight compounds during the distillation. High sulfur content in petroleum products is generally considered harmful in most petroleum products and the removal of sulfur compounds or their conversion to less deleterious types is an important part of refinery practice.

2.1.3   Metal compounds in Petroleum

In a refinery, the bottoms of the crude oil fractionation column, also known as residuum, contains a high proportion of metal contaminants along with sulfur and nitrogen. In crude oils, nearly one half of the elements in the periodic table have been identified as trace elements. Of these, the most abundant and problematic metals are vanadium and nickel. Contents of trace metals Ni and V are generally orders of magnitude higher than other metals in petroleum. Although these metallic constituents are present in small amounts, their removal is of considerable interest in petroleum industry [Agrawal *et al.* 1984].

Minute amounts of iron, copper, and particularly nickel and vanadium in the charging stocks for catalytic cracking affect the activity of the catalyst and result in increased coke and gas formation. Vanadium and nickel compounds cause major problems in hydrodesulfurization (HDS). These metal compounds deposit on and deactivate the

hydrodesulfurization catalysts, which have to be replaced. In high temperature power generators, such as oil fired gas turbines, the presence of metallic constituentslike vanadium in the fuel leads to ash deposition on turbine rotors, reducing clearances and disturbing their balance [Tamm *et al*, 1981].

A part of the metallic constituents of crude oil exists as inorganic water-soluble salts, mainly as chlorides and sulfates of sodium, potassium, magnesium and calcium. They can be removed using desalting operation. More important are the metals which are present in the form of water soluble organometallic compounds. Vanadium, nickel, copper and iron are present as oil-soluble organic compounds, capable of complexing with pyrrole compounds. Depending on the origin of the crude oil, concentration of vanadium commonly varies from 8 ppm (by weight) to 1200 ppm, while that of nickel commonly varies from 4 to 150 ppm.

Vanadium and nickel in petroleum exist either as metal porphyrins or as non-porphyrin metal complexes. The basic skeleton of these porphyrin compounds is porphine($C_{20}H_{14}N_4$), a closed ring of four pyrrole groups bridged by methane carbon atoms. The metalloporphyrins are formed by the chelation of a metal ion into the center of the porphyrin structure, with displacement of two protons from the pyrrolic nitrogen atom. Nickel is present in petroleum as Ni^{2+} and it sits in the plane of the porphyrin. Vanadium is present as vanadyl, VO^{2+}, the oxygen is perpendicular to the porphyrin plane and vanadium atom lies 0.048 nm above the porphyrin plane. The basic porphine structure is a plane of 0.8-1.0 nm diameter. Non-porphyrinic compounds which are present in the crude oil are however poorly characterized.

The metalloporphyrins are the best characterized metalcompounds in oil, and are natural choices for modelcompounds for investigations. Etioporphyrins (four methyl and four ethylsubstituents on the pyrrole rings) and octaethylporphyrinscomprise up to 50% of the metalloporphyrins in oil.Tetraphenylporphyrins (on the methine bridges) have notbeen identified in oil, but may be representative of highlyaromatic components in petroleum asphaltenes. Typical nickel compounds present in the heavy oil are shown in Figure 2.1[Wei, 2008]**.**

Ni octaethylporphyrin
(Ni OEP)

Ni tetraphenylporphyrin
(Ni TPP)

Ni etioporphyrin
(Ni EP)

Ni tetra-(3-methylphenyl)-porphyrin
(Ni T3MPP)
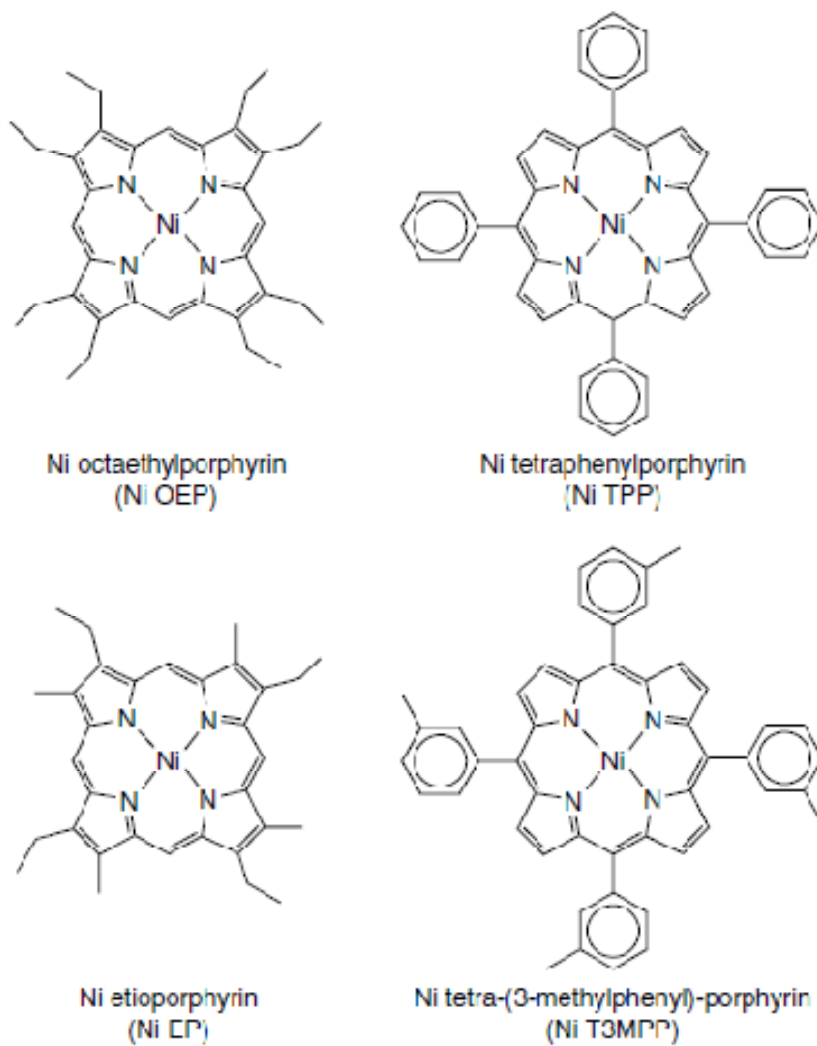
Fig 2.1 : Typical nickel porphyrins present in crude oil (Wei 2002).

2.2 HYDROTREATING REACTIONS

2.2.1 Hydrodenitrogenation

HDN is mainly used for lowering the nitrogen content in transportation fuels todiminish the emission of NOx from burning, and preventing downstream acidiccatalysts in refineries from being poisoned. At the same time, sulfur, metals, andunsaturated compounds are removed. Among hydrotreating reactions, HDN isreceiving more and more attention, because of the increasing interest in convertingpetroleum residua, coal, shale, and tar sands, which contain higher concentrationnitrogen, to liquid fuels. There are increasing demands for more clean and light fuelssuch as gasoline, kerosene, diesel and less heavier oils and also more stringentenvironmental regulations. Therefore, processing of more heavy feedstockssuch as vacuum gas oil (VGO), coker gas oil, residue, and light cycle oilproduced from VGO, residue and other sources of oils becomes important. Thusthe removal of sulfur (HDS) and nitrogen(HDN) are necessry. When processing heavier feedstocks, HDN is relatively more importantbecause the concentration of nitrogen-containing compounds in the heavier feedstocksis much higher than that in the straight run distillates. Usually acidic catalysts suchas those used for catalytic cracking of theheavier feedstocks are easily poisoned by nitrogen-containing compounds andpolyaromatics, especially the basic nitrogen-containing compounds.In order to develop new, effective HDN catalysts, further investigations on HDN processes and catalysts are still required.

Due to increased interest in processing heavy feeds, hydrodenitrogenation (HDN) of a variety of model compounds has been studied. Prins *et al.*,2001 have reviewed different aspects of HDN reactions. A comprehensive review of the HDN of various model compounds has been published by Furimsky *et al.*,2005.

Some of the earlier studies on HDN were carried out in the absence of H_2S or compounds that generate H_2S such as carbon disulfide or dimethyl disulfide. The catalysts may get reduced under the flow of hydrogen especially at higher pressures. Thus the results obtained may not be the characteristics of those obtained under industrial processing conditions. Under such industrial conditions H_2S will always be present from the HDS of the sulfur compounds in the feed because of high HDS conversion under HDN conditions.

Ahuja *et al.* , 1970 studied the activity and selectivity of presulfidedhydrotreating catalysts and evaluated their activity for many combinations of metal oxides and supports. They concluded that Ni promoted catalysts were better than Co promoted catalysts as Ni enhanced hydrogenation. Removal of nitrogen heterocyclic compounds takes place via hydrogenation of the heterocyclic ring containing nitrogen followed by breaking of the C-N bond (hydrogenolysis).

Among the different nitrogen compounds present in the oil, Quinoline has been used in this study as a model compound because it has many advantages over other nitrogen-containing hydrocarbons. Due to the bicyclic nature of the quinoline molecule, all the reactions which take place in industrial HDN occur in the HDN reaction network of quinoline as well viz. hydrogenation of the aromatic heterocyclic ring, hydrogenation of the phenyl ring and breaking of aromatic and aliphatic C-N bonds.

In principle there are two ways of the removing nitrogen atom inquinoline (Q), via o-propylaniline (OPA) or via decahydroquinoline (DHQ). In the first path, the heterocyclein quinoline (Q) is hydrogenated to 1,2,3,4-tetrahydroquinoline(THQ1) followed by ring opening toOPA. OPA is subsequently hydrogenated to PCHA,and the nitrogen atom is removed from PCHA byelimination.Inthe second HDN path, quinoline is fully hydrogenatedto DHQ which then reacts to PCHA and on to hydrocarbons. The reaction mechanism for the HDN of quinoline (Q) is shown in the Figure 2.2
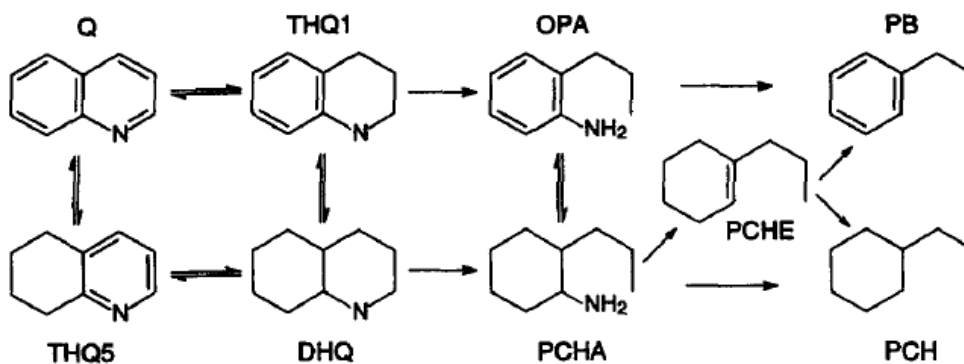
Figure 2.2 : Hydrodenitrogenation of quinoline (Q)

2.2.1.1 Effect of Partial Pressure of Hydrogen:

Effect of partial pressure of hydrogen and severity of process conditions on the HDN of basic and non-basic compounds from actual gas oil feedstock was studied by Frost and Jensen et al. ,1973. Conversion of non-basic compounds was found to be strongly dependent on the conversion of basic compounds.

Lee and Gioia et al , 1986 made a detailed study of hydrogen pressure on the HDN of quinoline. They varied the reaction pressure over a wide range, from 1.05 MPa to 15 MPa. They found that hydrogenolysis reactions were virtually pressure independent while the hydrogenation reactions increased with pressure. The effect of the hydrogen pressure on the over all rate of HDN depended on whether the hydrogenation or the hydrogenolysis step was rate controlling. They observed that for quinoline, as pressure was increased the rate of nitrogen removal also enhanced, suggesting that the hydrogenation was the rate controlling step.

Machida *et al.* ,1999 studied the effect of hydrogen pressure in the presence and absence of hydrogen sulfide during the HDN of quinoline. HDN of quinoline became enhanced as hydrogen partial pressure increased. Weakly adsorbed 1234-tetrahydroquinoline (1234-THQ) and *o*-propylaniline (OPA) were the main hydrogenatedintermediates with hydrogen sulfide,while strongly adsorbed and decahydroquinoline(DHQ) was main hydrogenated intermediate in the absence of hydrogen sulfide.

2.2.1.2 Metal oxides as catalysts for hydrotreating processes:

Mo or W based catalysts promoted by Co or Ni supported over γ-Al_2O_3 has been widely used in commercial HDN processes. There is an increasing trend in recent times to explore possibilities of using other metals for improving catalytic activity in HDN processes. Although Ni-Mo and Co-Mo catalysts have been used for a long time, the search for more active catalysts continues.

Pecoraro and Chianelli et al., 1981 were the first to investigate systematically I, II, and III row transition metal sulfides as catalysts. They showed that the unsupported sulfides of ruthenium, osmium, rhodium and iridium have much higher activities than those of Mo and W for the HDS of dibenzothiophene. The same type of study over transition metal sulfides was carried out by Eijsbouts*et al.*, 1988, 1991   for HDN reactions. They

demonstrated that Mo and W were not the most active metal sulfides for HDN. In the HDN of quinoline, hydrogenation was the rate determining step and the order of activity for equal molar amounts of transition metal sulfides supported on active carbon followed the order

Ir > Os > Pt > Re > Rh> Pd >Ru > Mo >W

Rangwala *et al.* ,1990 compared the performance of Ni-Mo and Ni-W catalysts for HDN of quinoline. They found that Ni-Mo catalysts with an optimum Ni/Mo ratio of about 0.24 showed better performance than Ni-W catalysts.

Metal carbides and nitrides have also been tried as catalysts for hydrotreating reactions. Schlatter *et al.*, 1988 studied the HDN of quinoline in autoclaves under industrially realistic conditions and found that activity of these catalysts was comparable to commercially sulfided Ni-Mo/Al$_2$O$_3$. Later Ramanathan *et al.*, 1998 studied several unsupported metal carbides and nitrides (Ti, V, Nb, Mo & W) as catalysts for HDS of dibenzothiophene and HDN of quinoline. Mo$_2$C showed good HDN activity. However, metal carbides and nitrides are not yet being used commercially. Presence of sulfur in the feed was found to have detrimental effect on the catalysts.

2.2.1.3 Effect of additives:

Effect of additives, such as phosphorus and fluorine,on activity of hydrotreating catalysts have been investigated by many researchers. It was found that addition of phosphorus resulted in better dispersion of molybdenum and nickel, changes in MoS$_2$ morphology, change in acidity of the support, chemical modification of active sites such as Mo, Ni (or Co), better resistance to coke formation during hydrotreating because of decreased acidity of the γ-Al$_2$O$_3$ support surface (Fitz and Rase *et al* 1983), and increased C–N bond cleavage due to an increase in the surface acidity of the support (Eijsbouts *et al* 1991).

In general, the influence of phosphorus depends on its quantity. At high loading, the presence of phosphorus usually leads to negative effect on HDN reactions by decreasing the surface area and by the modification of pore structure and possibly due to decrease in the dispersion of the active phase. Jones *et al.* ,1995 have reported that the addition of 1-3 wt.% phosphorus to Ni-Mo based alumina gave the maximum activity for gas oil and quinoline HDN, corresponding to an optimized surface acidity.

Liu *et al.* , 2004 studied the effect of phosphorus and fluorine on HDN of quinoline using Ni-Mo/Al$_2$O$_3$ catalyst. It was found that phosphorus was helpful in generating moderate to strong acidic sites as well as dispersion of Mo and the formation of active phases. Therefore, phosphorus promotes the hydrogenation of aromatic rings and hydrogenolysis activity of C-N bonds. Fluorine was found to generate weak to moderate acidic sites and better dispersion of Mo but was found to inhibit the formation of active sites. Addition of fluorine was found to be detrimental for hydrogenation of aromatic rings as well as hydrogenolysis of C-N bonds; thus, it was concluded that fluorine doesn't act as promoter.

2.2.1.4 Effect of Support:

Besides the active metals and promoters, support also plays an important role in HDN catalysis. Recently, research has focused on the development of other supports that can provide better dispersion of the active phase and better metal support interaction for achieving higher activity. The acidic and basic properties of the support also some time play vital role in achieving these objectives. Among the several supports, which have been investigated for hydrotreating processes the most important are oxides, mixed oxides, carbon, zeolites and mesoporous materials. These supports have been used either alone or mixed with alumina.

Different supports have been used to study HDN reactions. Silica was used as support to study nature of sulfided Mo phase on the support because of its inert nature and lesser interaction with the sulfided phase (Rives *et al.* , 2001). Carbon also has been used as support for HDN reactions. Due to microporosity, utilization of carbon materials as supports, however, has been restricted. In addition to diffusion limitations, carbon materials were found to have poor crushing strength, low bulk density and lower surface area. Apart from alumina, oxide supports such as TiO$_2$ and ZrO$_2$ have also been studied for HDN reactions.

Besides silica, carbon and metal oxides, various zeolites such as Y-zeolite, mordeniteand ZSM-5 have also been investigated for their activity in hydrotreating reactions.(Furimsky et al., 2005)

2.2.2 Hydrodesulfurization:

HDS has long been a major catalytic process. One of its main purposes is the removal of sulfur from naphtha reformer feedstocks, another is removal of sulfur from heavier fractions to minimize emissions of sulfur oxides from refineries and power plants. Stringent environmental regulations are exertingpressure to reduce the maximum allowable sulfurcontent in diesel. In most advanced countries, theallowable limit on diesel sulfur has been restricted to 50wppm or less.The molecules, which need to be removed for bringing down the sulfur content from 300- 500 wppm to a level of <50 wppm, are mainly the refractory dialkyldibenzothiophenes.

Amongst the model compounds, HDS of dibenzothiophene (DBT) and 4,6dimethyldibenzothiophene (4,6-DMDBT) has been widely studied. Several authors have proposed mechanisms for HDS of these model compounds. Houalla et al., 1978 proposed a detailed network for dibenzothiophene HDSon the basis of data from two laboratory reactortypes (fixed bed and batch reactor). The mechanism is shown below in Figure 2.3.
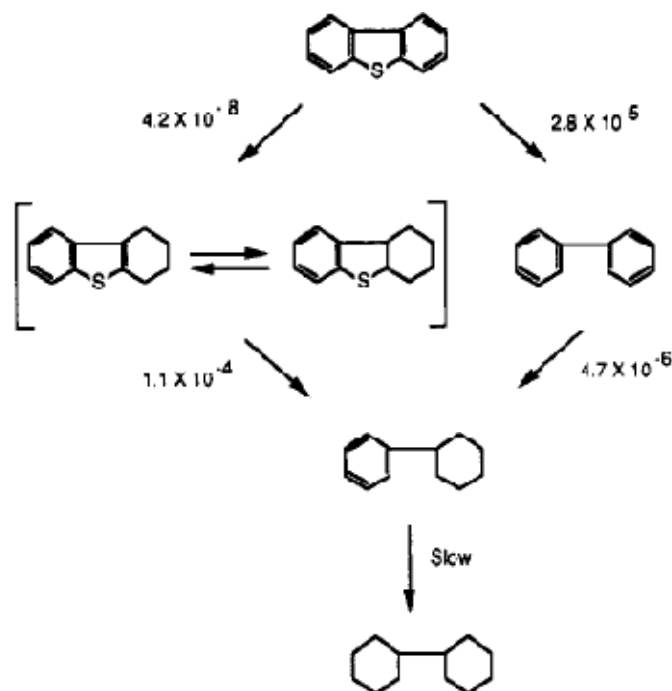
Figure 2.3 :Reaction network for dibenzothiophene proposed by Houalla *et al ,.*1978.

From the above scheme it is evident that HDS of DBT proceeds through two reaction paths: (1) direct elimination of sulfur to form the corresponding biphenyl (BPH) and (2) partial hydrogenation followed by sulfur removal to form cyclohexylbezene (CHB).

In the case of dimethyl dibenzothiophene, the position of alkyl groups plays an important role in controlling the reactivities of these molecules. For the dimethyl series, theease of desulfurization over a CoMo/Al$_2$O$_3$ catalyst is reported to be in the order:

2,8-DMDBT > 3,7-DMDBT > 4,6-DMDBT

revealing the the lowest rate for 4,6-DMDBT. The electronic effects of the alkyl groups are knownto be responsible for the relatively higher activity of 2,8-DMDBT. The primary reason for the poor reactivity of 4,6-DMDBT has been attributed to the steric hindrance of the methyl groups, which makes the sulfur atom inaccessible to the active sites of the catalyst.As a result, the HDS of 4,6-DMDBT does not tend to follow the direct desulfurization route typical of other sulfur compounds.

Bej *et al.* ,2004 in their review have summarized different possible routes for HDS of 4,6-DMDBT. The routes are shown in Figure 2.4.

Except direct desulfurization (DDS) all the routes aim at removal of steric hindrance of the methyl groups present at 4 and 6 positions. The effect of steric hindrance can be minimized or eliminated by hydrogenative and non-hydrogenative routes respectively. Hydrogenative route involves hydrogenation of the phenyl ring imparting flexibility to the methyl group. On the other hand non-hydrogenative routes involve isomerization, dealkylation of methyl groups or C-C bond scission.

Properties required in the catalysts are the hydrogenation function, which is provided by Ni, W, Pt, Pd, Ru etc., while reactions like isomerization, dealkylation and C-C bond scission require acidity function.
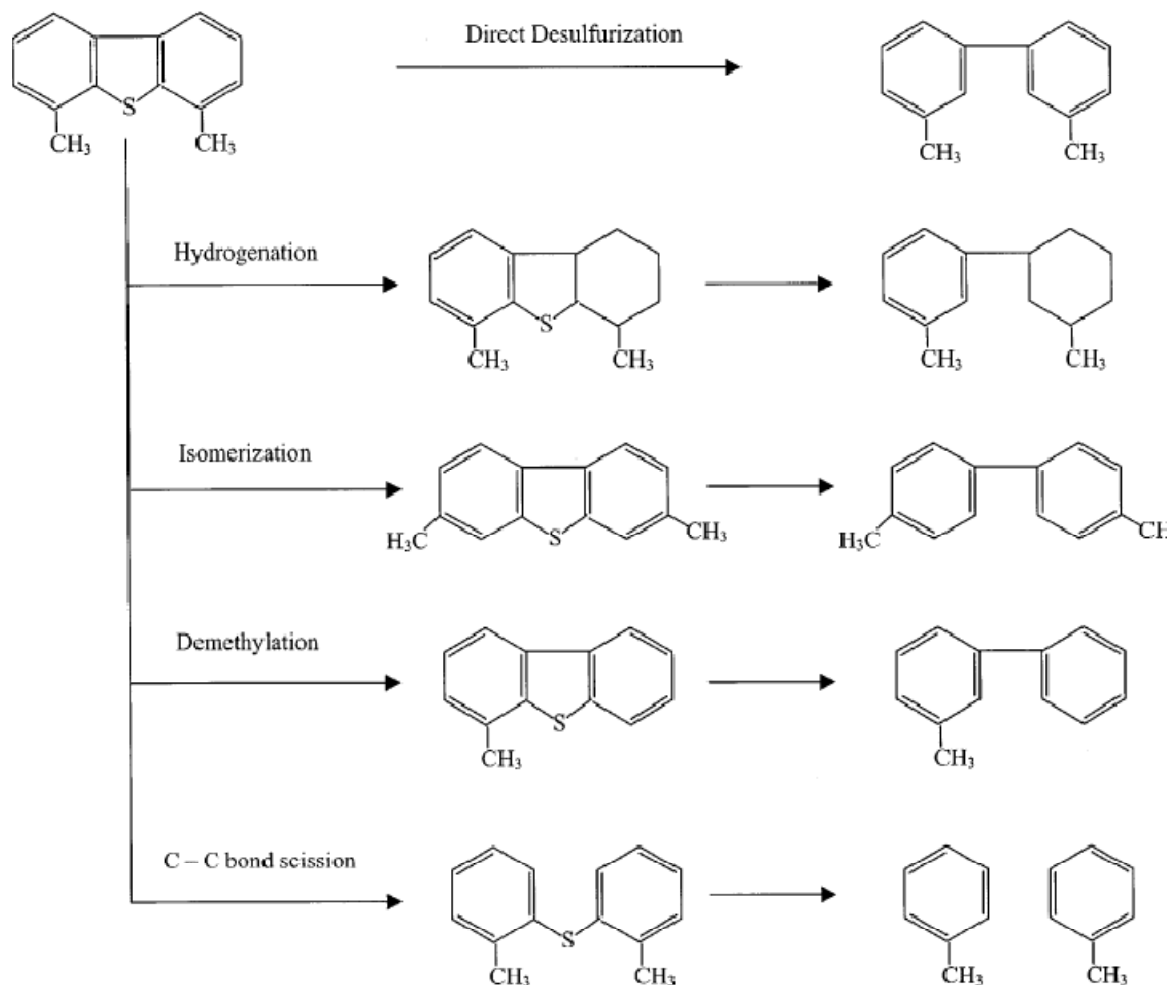
Fig 2.4 : Different routes for HDS of 4,6 DMDBT

2.2.2.1 Effect of Hydrogen and Hydrogen Sulfide Partial Pressure:

Kim *et al.* ,2005 studied the kinetics of HDS of DBT and 4,6-DMDBT using Ni-Mo catalysts supported on alumina. The reaction order of the overall HDS reaction with respect to hydrogen pressure was 0.6 for DBT and 1.1 for 4,6-DMDBT. Thus, the HDS of 4,6-DMDBT was found to be more hydrogen dependent compared to HDS of DBT.

The effect of hydrogen sulfide partial pressure on Ni-Mo catalysts supported on alumina inthe HDS of DBT and DMDBTwas studied by Kabe *et al.* ,2001. HDS rates of both these model compounds were found to decrease with increase in partial pressure of H_2S. HDS of DBT was found to be more inhibited by the presence of H_2S compared to that of 4,6 DMDBT. H_2S was found to possess agreater retarding effect on the direct desulfurization pathway.

2.2.2.2 Effect of Promoters:

Kwak *et al.* ,1999 studied the effect of phosphorus addition on HDS of DBT and 4,6 DMDBTon Co-Mo/alumina. Addition of phosphorus resulted in increasing the dispersion of molybdenum and Bronsted acidity of the support. In both the cases conversion was found to increase. In the case of HDS of DBT, addition of phosphorus favoured HDS by the hydrogenation route rather than direct desulfurization route. On the other hand, an opposite trend was observed in HDS of 4,6-DMDBT. In the case of methyl substituted dibenzothiophene, HDS was more pronounced by DDS route compared to hydrogenation route. This was attributed to enhanced acidity of the support. Conversion was found to increase at a phosphorus loading of 0.5 wt %.

Kwak *et al.* (2000), Kim *et al.* (2003)studied the effect of fluorine addition on HDS of DBT and 4,6 DMDBT over Ni-Mo/alumina. Addition of fluorine resulted in increasing the dispersion of molybdenum and increasing the acidity of the support. In the HDS of DBT, hydrogenation was the more favoured route compared to direct desulfurization, while in case of substituted DBT, DDS was the more pronounced route compared to hydrogenation. In the case of HDS of DBT, activity of the catalyst was found to be a maximum at afluorine content of 0.5 wt % while in case of substituted DBT, HDS activity was found to increase upto a fluorine content of 5 wt%.

2.2.2.3 Effect of Support:

Support plays an important role in controlling the acidic property of the catalyst. Different metal oxide supports such as TiO_2, Al_2O_3, ZrO_2 have been investigated. Various types of zeolites have been added toalumina for increasing its acidity. An increase inacidity is expected to enhance the isomerization anddealkylation of the alkyl groups present in 4,6-DMDBT. A mixture of Y-zeolite and alumina was found to favourthe DDS route during the HDS of 4,6-DMDBT due to enhanced acidity. (Bej *et al.* , 2004).**A** mixture of ZSM-5 and alumina however showed a decrease in HDS activity and no change in product distribution during the HDS of 4,6-DMDBT; this may be due to the restricted diffusion of the bulkier 4,6-DMDBT molecule within the pores of the catalyst.

Apart from mixtures of different oxides and zeolites with alumina, zeolites and mesoporous materials as individual supports have also been investigated. (Bej *et al.* 2003).Carbon as a support also has been widely investigated by the researchers for the HDS of 4,6-DMDBT. (Farag*et al.* 2000, Sakanishi*et al.* 2000)

Most of the studies related to support modifications were done for the HDS of thiophenic and dibenzothiophene compounds. However, relatively less research has been conducted on HDS of substituted DBTs. As supports, Zeolites have not shown much promise. Mixed oxides and metal carbides (instead of sulfides), however, appear to be potentially useful.

2.2.3 Hydrodemetallation:

Many important catalysts used in the petroleum refining industry are based on alumina supports. In alumina supported catalysts, the active catalyst components remain dispersed to a large extent within the pores of the support. The pore size of the alumina support, therefore, plays an important role in influencing the activity of the catalyst, particularly for reactions involving large molecules.

Anchetya *et al.*, 2005 reviewed key aspects of hydroprocessing catalysts. These included physical properties, mechanical properties, shape & size of the catalysts. Textural properties such as pore volume and pore size distribution and mean pore diameter have to be optimized to maximize catalyst utilization. Catalysts with a high surface area and moderate pore volume were very active for HDS because of the efficient dispersion of the active metals in the pores. However, in the case of heavy feeds, these pores became gradually unavailable because they were deactivated by pore mouth plugging due to deposition of metals. On the other hand, catalysts with a small surface area and a large pore volume were less active because of a lower concentration of active sites. However, they were more resistant to deactivation by pore mouth plugging and their metal storage capacity was greater. Thus HDM conversion was found to be influenced by the average pore diameter (APD). Low HDM conversion for a low APD catalyst was caused by restricted diffusion of the large metal-containing molecules (porphyrins and/or metal chelating compounds) into the pores. There is an optimal combination of surface area and pore diameter giving the highest catalyst activity. The optimum may be different for different feeds and catalysts. An optimal pore size and volume distribution was found to be critical for hydroprocessing of high metal content feeds. For small pore diameter, most of the metals deposit on the external surface of catalyst particles and the diffusion into the interior of the catalyst becomes a rate-limiting factor. It is, therefore, expected that the tolerance of catalyst to metals will increase with increasing pore diameter. For the same surface area, bimodal catalysts were found to be more effective than unimodal catalysts. Because of a higher metal tolerance, bimodal and even polymodal catalysts were found to have a longer life and their metal storage capacity may approach 100% of the original catalyst weight.

Rana *et al.*, 2004 studied the effect of support preparation on hydrodemetallization of Maya crude oil. The effect of support (γ-alumina) preparation methods was compared. Pure alumina supports were prepared by using different preparation methods such as urea (γ-

Al$_2$O$_3$-u), ammonium carbonate (γ-Al$_2$O$_3$-acs) and ammonia (γ-Al$_2$O$_3$-am) as hydrolysing agents. Mo supported catalysts were prepared by incipient wetness method. The Co promoted catalysts were also prepared by a sequential impregnation procedure on Mo-loaded catalysts. A Maya crude oil - diesel (50/50 (w/w) mixture was used as HDM feed. Supports prepared by urea hydrolysis and ammonium carbonate routes were found to provide better pore size distribution as well as higher pore volume. The support prepared using ammonia only revealedpores in the meso-pore range and high surface area. The support preparation method influences pore size distribution and average pore diameter which, apparently, control catalytic activity. Catalysts with a larger pore size distribution (CoMo/γ-Al$_2$O$_3$-u and CoMo/γ-Al$_2$O$_3$-acs) had better HDM activity and more stable activity with time-on-stream.

Maity *et al.*,2003 also studied catalysts for the hydroprocessing of Maya heavy crude oil. Authors studied five different catalysts by loading various active metals on an alumina support. Co-Mo (A), Ni-Mo (B), Co-W (C), Ni-W (D), P-Co-Mo (E) supported on alumina were used in the studies. The amount of active metals loaded was 4 wt % in all the five cases. Catalysts A and C showed better activity for HDM than catalysts B and D indicating that Co promoted catalysts show better performance for HDM than nickel promoted ones. Also the HDM activities of the catalysts were in the order: Co-Mo (A) > Co-W (C) and Ni-Mo (B) > Ni-W (D) indicating that Mo was a more active metal for HDM than W. Catalyst E with P-Co-Mo combination revealedthe highest initial activity for HDM. Although the initial activity of the P containing catalyst was high, a rapid fall in activity was observed with time. This deactivation was due to coke deposition. In order to reduce coke formation, Li metal was doped into the catalyst. Li doped catalysts did not show any significant difference in activity.

Rankel *et al.* ,1993 , Chen *et al.* ,1999,Anchetya-Juarez *et al.* ,2001,Santes *et al.* ,2005 studied hydrodemetallation of nickel and vanadium compounds using actual crude oil feedstocks.

Earlier studies were based on the hydrodemetallation reactions using model compounds. Three types of nickel or vanadium porphyrinshave been usedfrequently as model compounds in HDM studiesbecause they are representative of the real molecules in thecrude, they are: etioporphyrins (Etio type), tetraphenylporphirins(TPP) and tetra(3 methyl-phenyl)porphyrins.

Hung and Wei et al. ,1980 reported first order kinetics for hydrodemetallation using nickel and vanadium porphyrins as the model compounds. The experiments were conducted

in a 1 L autoclave using reduced Co-Mo catalysts supported on alumina support. Agarwaland Wei (1984) reported first order kinetics for thehydrodemetallation reaction using nickel and vanadium etioporphyrins in a trickle bed reactor using reduced Co-Mo catalysts supported on alumina support. Ware and Wei (1985) studied the hydrodemetallation of nickel porphyrins using unsulfided Co-Mo/alumina catalysts. Porphyrins were found to initially hydrogenate forming intermediate species, which subsequently react via hydrogenolysis steps to deposit metals on the catalyst surface.

Chen and Massoth et al., 1988 studied the HDM of vanadium porphyrins and Ni-TPP using sulfide catalysts in a 1 L autoclave reactor. Higher hydrogen pressure and higher temperatures were found to give higher hydrodemetallation activity. The generalized reaction scheme for Ni-TPP is shown in the Figure 2.5.Bonne et al. (1995, 2001) studied the HDM of nickel and vanadium tetraphenylporphyrins in the presence and absence of the catalysts. In both cases nickel and vanadium porphyrins were observed to undergo sequential HDM through hydrogenation reaction followed by hydrogenolysis or ring fragmentation to deposit metals on the catalyst.
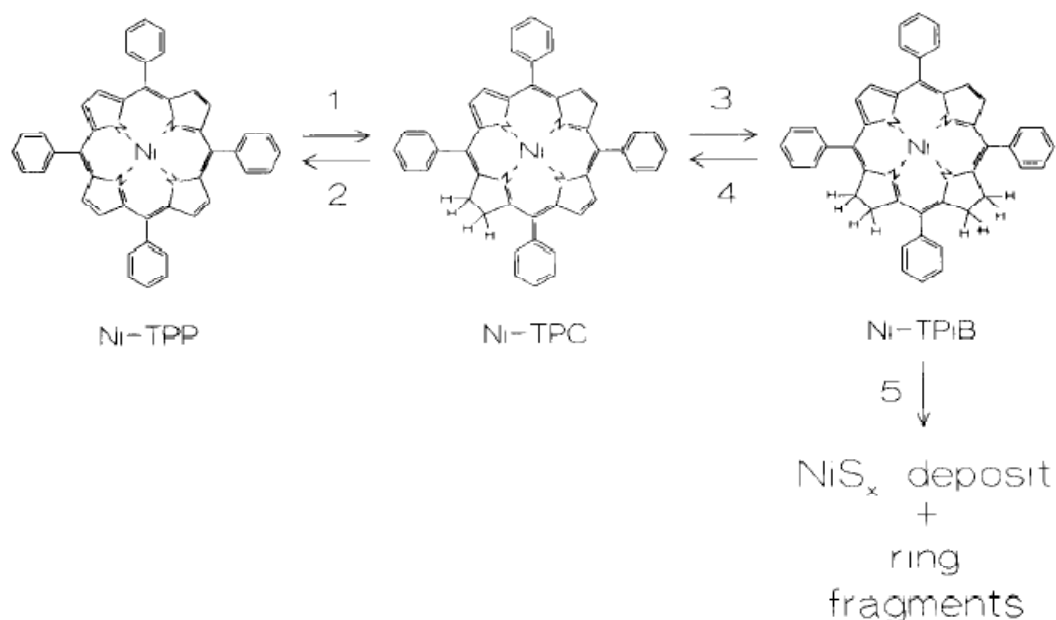
Figure 2.5 : Hydrodemetallation of Ni-TPP

Garcia-lopez *et al.* (2005) carried out the HDM of nickel tetraphenylporphyins (Ni-on TPP) over Al_2O_3-TiO_2 supported-Mo catalysts in a batch reactor. A mechanism similar to the one shown above was observed. However, the rate determining step was found to be

27

hydrogenation instead of hydrogenolysis or ring fragmentation. This was attributed to the higher acidity of the supports compared to alumina supports.

In a majority of the publications, HDM studies were done using unsulfided or sulfided Co-Mo catalysts supported on alumina. Ni-Mo catalysts were not studied in detail; also supports other than alumina were not investigated in detail.

2.3 Catalyst Structure:

Catalysts used in industrial hydrotreating processes generally consist of Mo loaded on alumina with Co or Ni as promoters. The important factors which affect the activity of the catalysts are impregnation, drying, calcination and sulfiding steps. Co or Ni ions interact strongly with the alumina surface and after calcination form a surface spinel with Co^{2+} and Ni^{2+} in octahedral or tetrahedral holes. At high metal loading, NiO or Co_3O_4 crystallites are formed on the support surface.

Oxidic precursors which are formed during sequential impregnation, drying and calcinations can be transformed into the actual hydrotreating catalysts by sulfidation in a mixture of H_2 and H_2S. On sulfidation, MoS_2 species are formed on the surface of alumina. MoS_2 has a layered structure with weak interaction between the sulfur atoms of the successive layers. Co and Ni which are used as promoters, after sulfidation may be present as Co_9S_8 and Ni_3S_2 crystallites, as cobalt or nickel ions at the edges of MoS_2 crystallites (Co-Mo-S or Ni-Mo-S phases) or as cobalt or nickel ions in the tetrahedral support lattice. Figure 2.6 shows the schematic representation of the active sites on an alumina support.
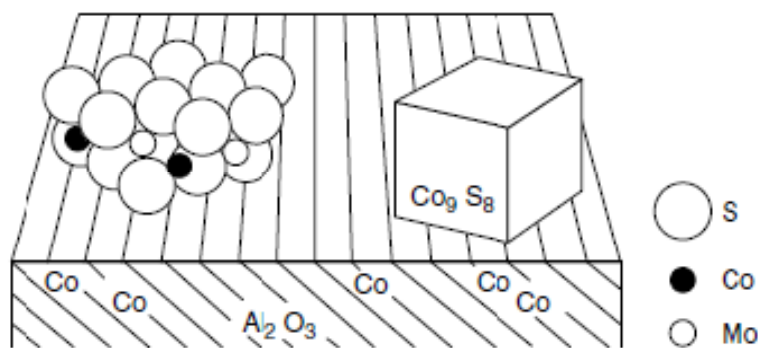
Figure 2.6 : Forms of promoter species present in sulfide catalysts

Co/Mo or Ni/Mo ratio is important in determining the catalytic activity. At low cobalt loadings and mild sulfiding temperatures, all the cobalt atoms can be positioned around MoS_2 edges. Initially the catalytic activity increases with increase in Co/Mo or Ni/Mo ratio. At high cobalt loadings, however, all the edge sites are occupied and additional Co atoms have to be located on other Mo-sites or as Co_9S_8 crystallites on the support. Since the Co_9S_8 species have low catalytic activity and cover MoS_2 species, catalyst activity reduces at higher promoter loadings. The optimum Co/Mo or Ni/Mo ratio is 0.3-0.5 for maximum activity.(Craje *et al.*1992)

Candia *et al.* (1981) proposed that, there are two forms of Co-Mo-S and Ni-Mo-S structure, with Co or Ni ion occupying the edge site. The more active phase was called Co-Mo-S II while the less active phase was called Co-Mo-S I. The type I structure was said to be bonded with the support via Mo-O-Al linkages while in case of type II structures such linkages were very low in number. Type I was less active compared to type II species due to steric reasons. Catalyst-support linkages of type-I probably hinder the approach of reactant molecules to the active site.

Daage *et al.* (1994) proposed a "Rim-edge" model to differentiate between the active sites. Fig 2.7 shows the schematic of the "Rim-edge" model proposed by Chianneli *et al.* According to this model, the active MoS_2 structure consists of two sites, edge sites and rim sites while the basal plane is considered to be inactive. Active centres for hydrogenation reaction lie on the rim sites while those for hydrogenolysis or C-S bond rupture lie on the edge sites. Stacking height for the given diameter of MoS_2 slab determines the ratio of rim to edge sites. Ratio of the edge to rim sites alters the selectivity. Use of promoters like Co or Ni which occupy the edge sites, reduces the difference in the reactivity of edge and rim sites by preferentially enhancing the activity of the edge sites.
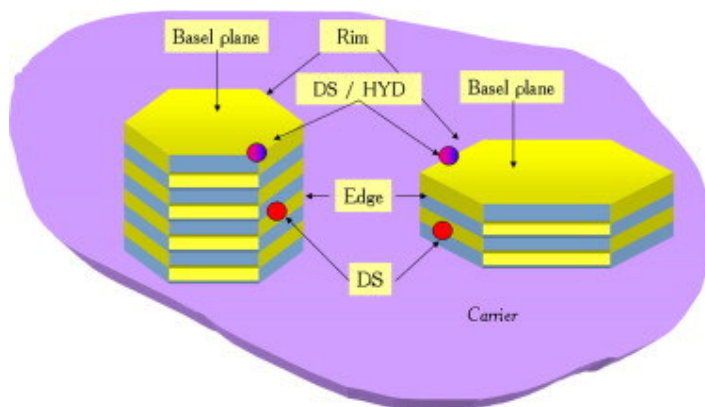
Figure 2.7 : "Rim-edge model" Daage et al (1994)

2.4 Mesoporous Catalytic Systems:

In porous solids, the reactant molecules interactnot only on the surface but also inside the porewalls of the materials. Due to this property ofenhancement in reaction sites, they are of greatimportance. Porous solids are classified in to threegroups based on their pore sizes, microporous materials (d <2 nm), mesoporous materials (2 nm< d >20 nm) and macroporous materials (d>20 nm). In recent years, there has been an urge to use heavier petroleum fractions and biomass to produce chemicals and bring about energy conversions. Small pore sizes of microporous materials (zeolites) are inadequate, since they do not allow the passage of large molecules and cause diffusivity problems for large molecules. Mesoporous materials can very well be used for this purpose. Mesoporous materials can be classified into different types, eg. silicates, aluminophosphates, metal oxides and carbon.

2.4.1 Alumina:

Aluminas are extensively used as catalyst supports due to their favorable textural properties and intrinsic acid–base characteristics. In addition, these materials possess excellent thermal and mechanical stability. Although aluminium oxide existsin various structures, only three phases are of interest, namely the nonporous, crystallographically ordered a-Al$_2$O$_3$, and the porous microcrystalline η- and γ-Al$_2$O$_3$. In particular, γ-alumina, which has alarge surface area and a crystalline structure, is an importantcatalyst support in automotive and petroleum industries. Alumina supports with large surfaceareas, large pore volumes, narrow pore size distributions within the mesoporous range, as well as suitablesurface acidic–basic properties can often result in favorable enhancements in catalytic performances.

30

Different ways of synthesizing alumina using different precursors are shown in Figure 2.8.Alumina supports are made by thermal dehydration of $Al(OH)_3$ (gibbsite or bayerite) or AlOOH (boehmite). Aluminium is found in nature in the form of bauxite, an ore consisting of aluminium hydroxides, silica and other oxides. Depending on origin, the bauxite consists mainly of gibbsite, boehemite or diaspore. Alumina is extracted from the ore by treating it with NaOH, yielding a $Na_2Al_2O_4$ solution from which gibbsite is obtained by crystallization. Therefore gibbsite always contains alkali which is unsuitable for catalytic applications.

Alkali free aluminas are therefore prepared by hydrolysis of aluminium alcoholates, like $Al(OC_2H_5)_3$, which yields a gelatinous form of boehmite which is also called as pseudo-boehmite. Yet another preparation route starts from bayerite, formed by the precipitation of $Al(OH)_3$ from aluminium salts to which ammonia is added in solution. Bayerite forms at a high pH (about 12) and boehmite at more neutral pH values.
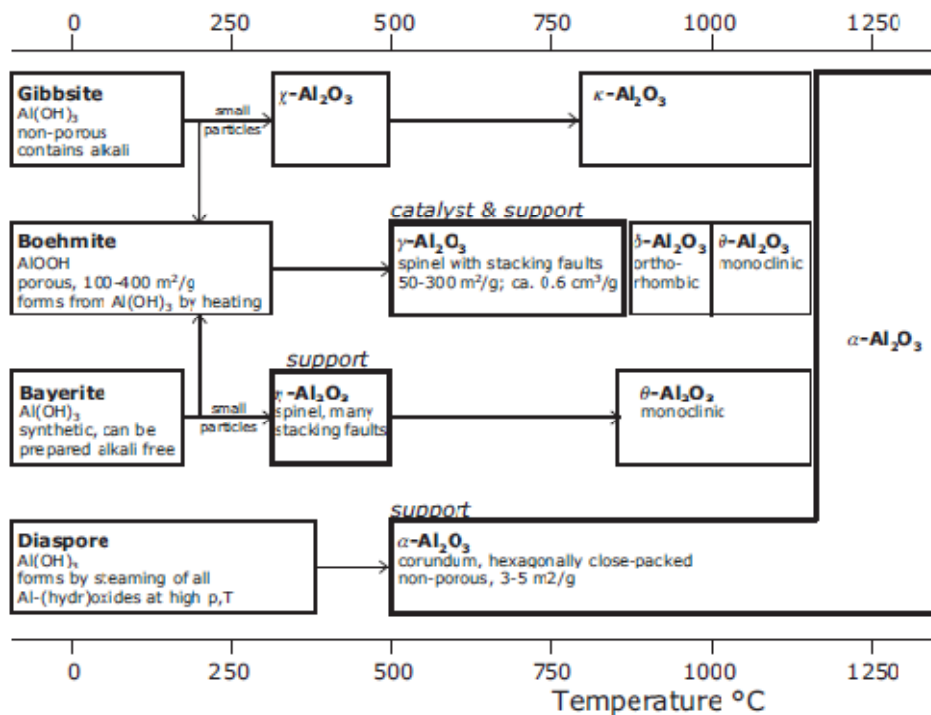
Figure2.8 : Different forms of Alumina (de Jong, 2008)

Alumina exists in several forms, among which only the α-form is highly crystalline.α-alumina is the most stable, least acidic and lowest surface area form of alumina. The others

are called transitional aluminas which have spinel like structures with different orders in which layers are stacked.

As a support, γ-Al_2O_3 offers high surface areas (50–300 m^2 g^{-1}), mesopores ofbetween 5 and 15 nm, pore volumes of about 0.6 cm^3 g^{-1}, high thermal stabilityand the ability to be shaped into mechanically stable extrudates and pellets. Thermal stability can be improved by addition of additives. Its surface contains several hydroxyls, between 10 and 15 OH per nm^2,the linear ones being Brønsted bases (H$^+$ acceptors), and the bridged ones Brønsted acids (H$^+$ donor).After dehydroxylation, the surface develops Lewis acidity (electronacceptor) on the uncoordinated Al$^{\delta+}$ sites. Thus γ-Al_2O_3 has in fact both Brønsted acidity due to the presence of surface hydroxyl groups and Lewis acidity at dehydrated aluminium sites.

Amongst all forms of transitional alumina γ-Al_2O_3 has been used widely as a support for reactions such as alkene and benzene hydrogenations, catalytic reforming, hydrotreating, methanol synthesis, water gas shift reaction etc. Because of its moderate acidity it has also found applications in reactions such as isomerization, cracking, hydrogenation and dehydrogenation.

2.4.2   Mesoporous Silica:

The essence for the construction of ordered porous materials is self-assemblyby which molecules (or parts of molecules) spontaneously organizeinto stable, structurally well-defined aggregates. By utilizing the self-assembling approach, a family of ordered mesoporous silicas, the pore size ranging from 2 to 50 nm, emerged in the early 1990s. The self-assembling process involves noncovalent or weak interactions. Most ordered mesoporous materials are derived from the thermodynamically stable and ordered aggregates spontaneously driven by non covalent interactions between molecules. These aggregates come from the cationic, anionic and non-ionic surfactants, neutral amines, block co-polymers or their mixtures.
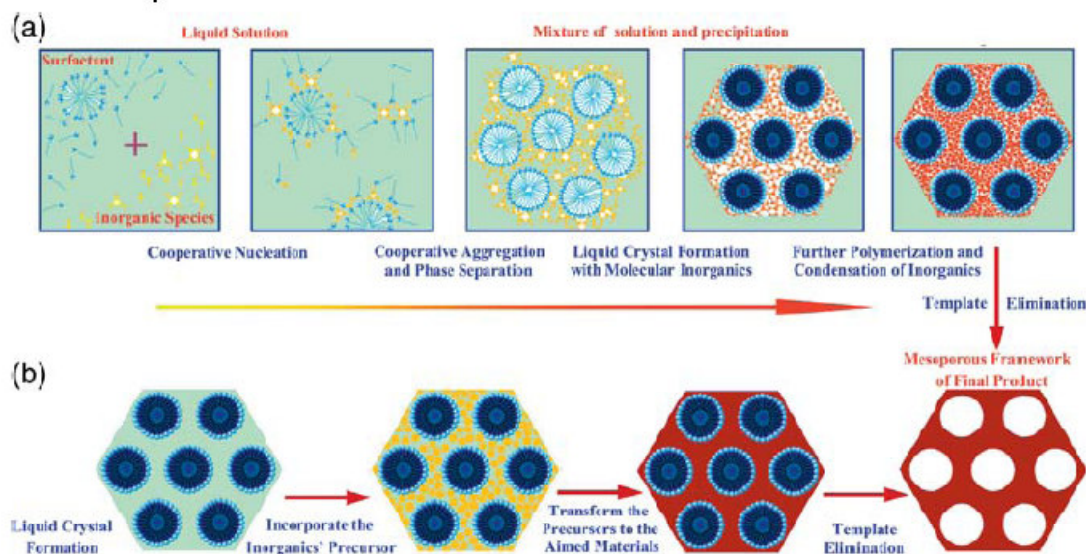
Figure2.9: Synthetic routes for the formation of mesoporous materials(de Jong, 2008)

There are two routes for the formation of mesoporous materials. Route A is the cooperative self-assemblyof surfactants and silica sources to form mesostructures, and the route B is a so-called ''true'' liquid-crystal template pathway. Route A occurs at low concentration of surfactant while route B is favoured at larger surfactant concentration. At the final stage, the aggregates are removed by calcination, extraction, microwave digestion, or oxidative decomposition. Pores are opened, the dimension, shape, and topology depending on the size and morphology of supramolecular aggregates.

Several tens of kinds of different ordered mesoporous silicates have been synthesized and named. However there are only fewer mesostructures. Most of the mesostructures belong to either hexagonal or cubic phases.2D-mesostructured silica with the hexagonal symmetry are most easilyproduced, the classical products being MCM-41, FSM-16, SBA-3, and SBA-15. The 3D-mesostructures possess anintergrowth of hexagonal close packing (*hcp*) and cubic close-packing (*ccp*)phases (SBA-2, SBA-7 and SBA-12), cubic bicontinuous structures(MCM-48, FDU-5, KIT-6), simple cubic structures (SBA-1, SBA-6, and SBA-11), face-centered cubic structures (FDU-12 and KIT-5), body-centered cubic structures (SBA-16). Among them, MCM-41, SBA-15, and MCM-48 are the extensivelyinvestigated mesoporous silica molecular sieves(de Jong, 2008).

2.4.2.1 SBA-15

After MCM-41, the second important 2D hexagonally mesostructured silica is SBA-15 molecular sieve, first reported by Zhao *et al.* in 1998. SBA-15 has a highly ordered 2D hexagonal mesostructure with a very uniform pore-size distribution.SBA-15 materialsprepared from P123 at 40–100 °C (hydrothermal temperature) have uniformpore sizes from ~6.5 to 10 nm. The pore-wall thickness is calculated to be 3.1–4.8 nm, much thicker than that of MCM-41, which results in higher thermal and hydrothermal stability.

The wall structure of SBA-15 is different from MCM-41, although the two materials have the same kind of symmetry. Triblock copolymers not only play the role of templates but also insert into silica frameworks with EO blocks and form organic–inorganic hybrid frameworks. After calcination, micropores or small mesopores are left in the frameworks and connections between the mesopores are generated owing to the removal of triblock copolymers. No diffraction peak assigned to these micropores is detected in XRD patterns due to the disordered arrangement. Nitrogen sorption techniques reveal pore sizes between 1 and3 nm. The intra-framework pore volumes contribute about 30% of total volume. Complementary porosity of SBA-15 can be retained to a significant extent even after calcination at 900 °C, but probably completely disappears at 1000 ∘C. Adding a cosolvent like ethanol and a small amount of salts manipulates the P123 micellar environment and hence eliminates the microporosity of SBA-15 after a microwave hydrothermal treatment.

SBA materials are obtained by sol-gel process involving hydrothermal treatment. At first a homogeneous solution of surfactant is obtained, to which silica precursors are added. Since the isoelectric point of silica is (pH) is 2 and hence a highly acidic solution is used (pH < 2) in order to get positively charged silica species. The mixture (surfactant solution, silica precursors and acid) is stirred at a particular temperature, which is determined by critical micelle temperature (CMT) and cloud point (CP) of the surfactant. The synthesis or gelation temperature should be such that it is above CMT and below CP of the surfactant. In synthesis, HCl is mainly used as acid catalyst as it takes less time to precipitate than other acids. The acid catalyst hydrolyzes silica precursors to form oligomers which in turn aggregate around a micelle through CSA. A high concentration of acid leads to faster polymerization but highly concentrated acid (>4 M) is not preferred. A low concentration of the acid catalyst favors a slow condensation of silicate species leading to a highly ordered material. The final gel is subjected to hydrothermal treatment. The precipitate obtained is filtered and washed; actually

washing is not necessary as volatile HCl can be removed with surfactant upon calcination. Since the synthesis is carried out in the presence of acidic medium only TEOS or sodium metasilicate can be used as silica precursors. For alkaline medium synthesis any silica precursors can be used. The mechanistic pathway for the formation of SBA-15 is shown in Figure 2.10.
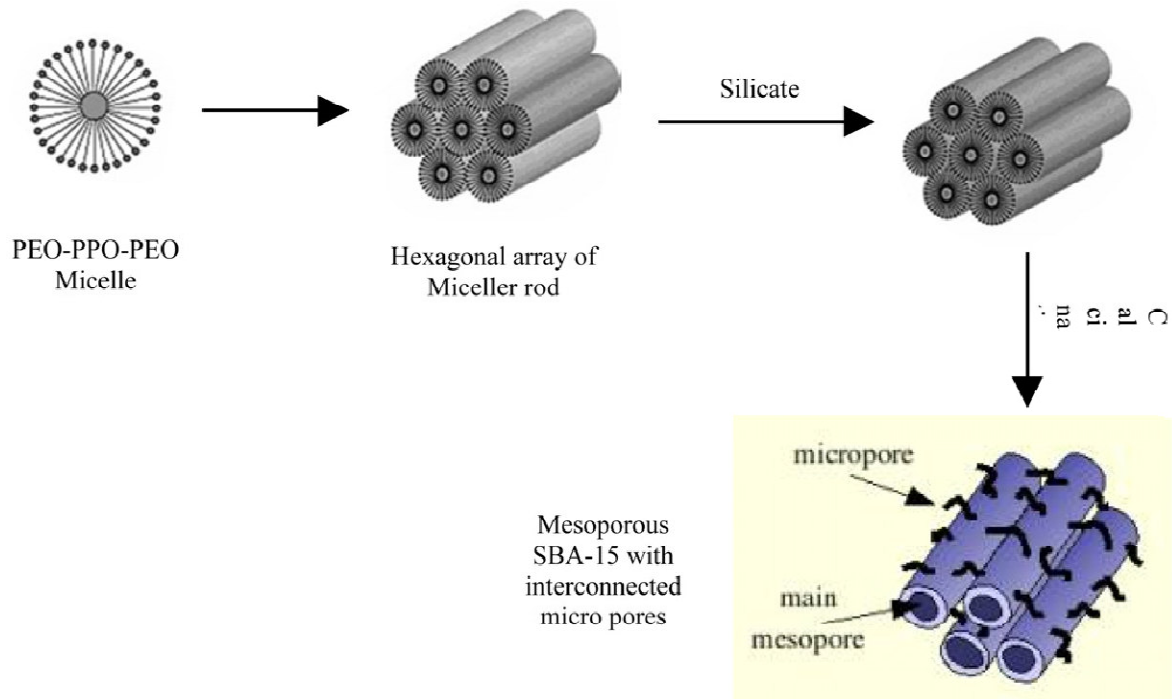
Figure 2.10 : Mechanistic pathway for the formation of SBA-15 material.(Zhao et al., 1998)

The high surface area and controlled large pore size of SBA-15 makes it a promising support for applications in oil refining involving large molecules.

CHAPTER III

EXPERIMENTAL

In this chapter, a description of the materials and methods used during the course of this work is presented.

3.1 Chemicals

Alumina hydrate (Pural SB, Sasol), acetic acid (Glacial, 100 %, Merck) were used as procured in the preparation of the alumina support.

Hydrochloric Acid (min 35 % GR, Merck), tetraethyl orthosilicate ($C_8H_{20}O_4Si$, MW = 208.33 g/mol, 99 % purity, Merck), Pluronic® P123 (PEG-PPG-PEG, MW ~ 5800, Sigma Aldrich) were used as procured in SBA-15 synthesis.

$(NH_4)_6Mo_7O_{24}.4H_2O$ (AR, Central Drug House (P) Ltd., India) and $Ni(NO_3)_2.6H_2O$ (Merck Specialities Pvt. Ltd., India), ammonia Solution (25 % assay, SRL) were used as procured in metal impregnation on the supports.

Quinoline (Q) (C_9H_7N, Reagent Grade 98%, Sigma Aldrich) was distilled under vacuum before use as a feed in hydrodenitrogenation reactions. The distillation was carried out carefully in order to avoid water ingress in the distilled quinoline. 1,2,3,4-Tetrahydroquinoline (1-THQ), ($C_9H_{11}N$, 98 % purity, Sigma Aldrich) was also distilled under vacuum carefully before using as a feed in hydrodenitrogenation reaction.

Decalin or decahydronaphthalene (98 % Purity, Sigma Aldrich), dibenzothiophene (DBT)($C_{12}H_8S$, 98 % purity, Sigma Aldrich), 4,6-dimethyldibenzothiophene (DMDBT) (98 % purity, Sigma Aldrich), 5,10,15,20 – tetraphenyl *21 H, 23 H* porphine (Ni-TPP) (Sigma Aldrich), paraffin oil (density 0.86-0.89 g/cc, kinematic viscosity $\geq$ 64 cS, Merck), dimethyldisulfide (DMDS) (CPCL), n-hexane (95 % purity, HPLC grade, SRL) were used as procured.

Commercial nitrogen and hydrogen (high pure) obtained from Indian Oxygen Limited was purified by passing the gas over dried silica gel to absorb the moisture.

3.2 Synthesis of Support:

3.2.1 Alumina

Extrudates (1/16") of alumina were prepared by peptization of alumina hydrate (Pural SB, Sasol) with a small amount of 2 wt% acetic acid in water, extrusion using a hand extruder, drying at room temperature (overnight) and at 393 K (12h), and finally calcining at 773 K (6 h).

3.2.2 SBA-15

SBA-15 was synthesized under hydrothermal conditions using the procedure outlined in Zhao *et al.* (1998). 4 g of Pluronic $^{®}$ P123 was dissolved in 40 ml of double distilled water and the mixture was allowed to stir for 90 minutes till the clear solution was obtained. 50 ml of 2 M HCl was added to the solution and the mixture was allowed to stir for 30 minutes. 9 gm of TEOS was added dropwise to the mixture and the mixture was kept for continuous stirring in an oil bath maintained at 313 K for at least 20 h. The white gel obtained after 20 h duration was transferred into a Teflon lined autoclave or polypropylene bottle and kept for hydrothermal treatment at 373 K for 48 h duration. The product after hydrothermal treatment was filtered, washed thoroughly with water and dried at 323 K for 6 h. Calcination was carried out in a tubular furnace under a continuous flow of air at 823 K for 6 h.

3.3 Preparation of the catalyst:

The impregnation of the supports with the Ni and Mo precursor salts was made by a wet impregnation method using aqueous solutions of nickel nitrate ($Ni(NO_3)_2.6H_2O$ and ammonium heptamolybdate (($NH_4)_6Mo_7O_{24}.4H_2O$). The pH was adjusted to ~11.0 using 25 wt% aqueous NH_3 solution. In the case of NiMo catalysts, both metals were impregnated simultaneously. The nominal composition of the catalysts was 4 wt.% of NiO and 15 wt.% of MoO_3. After metal impregnation, the catalysts were dried at room temperature overnight followed by drying in an oven at 393K for 12 h and calcined at 773K for 6 h.

3.4 Instrumentation

3.4.1 X-ray powder diffraction (XRD):

X-ray powder diffraction is used as the main characterization tool when solid materials are synthesized. This characterization technique can be used for samples having long range orders. It is used for phase identification, crystallite size measurement and unit cell parameter determination. For analysis, the sample is first powdered and carefully applied to the glass plate (sample holder), after which the plate is placed inside the X-ray powder diffractometer.

XRD patterns of the samples were recorded on Rigaku Miniflex (II) X-ray diffractometer using Cu K_{α} (λ= 1.5405 Å). Crystallite size can be calculated by X-ray line broadening using Debye-Scherrer equation (Cullity, 1978),

$$d = \frac{k.\lambda}{\beta.\cos\theta}$$

(3.1)

where, d is the crystallite size in nm, K is a numerical constant, 0.86; λ is the wavelength of radiation used; β is full width at half maximum in radians and θ is the Bragg diffraction angle in degrees, at the peak maximum. The unit cell parameter a_0 was found from the equation $a_0 = 2d_{100}/\sqrt{3}$. The peak height gives the intensity of the corresponding peak. A sum of the peak instensities of selected peaks is often used to characterize the crystallinity of the sample.

The XRD patterns were recorded at a scan rate of 3°/min, sampling width of 0.02° for the 2θ range of 5-90°. Low angle XRD patterns were recorded on Bruker D8 Advance Powder X-Ray Diffractometer at a scan rate of 1°/min, sampling width of 0.02° for the 2θ range of 0.5-8°.

3.4.2 Textural properties determination:

Textural properties of the catalyst such as pore size, pore volume. pore size distribution and surface area were found out by using nitrogen adsorption method. Nitrogen adsorption and desorption isotherms were obtained at 77 K on an ASAP2020 analyser

(Micromeritics, USA). All the samples were initially degassed at 373 for 2 h and at 423 K for 3 h under vacuum in the degassing port of the analyzer.

The specific surface area was calculated following the BET procedure. The pore size distributions of the materials were calculated from the desorption branch of the nitrogen isotherm following the BJH method.

3.4.3 Diffuse reflectance UV-Vis Spectroscopy:

Diffuse reflectance UV-Visible absorption spectra of the catalysts were recorded using a Thermo Scientific Evolution 600 spectrophotometer equipped with a Praying mantis diffuse reflectance accessory. 0 % baseline correction was done initially by placing the DRS accessory in the sample compartment followed by 100 % baseline correction using barium sulfate (spectral grade) as a reference. This was followed by UV-Visible spectroscopic analysis of the catalyst samples.

3.4.4 Transmission Electron Microscopy (TEM):

Transmission electron micrographs were recorded on a Philips CM20 model (200 kV). Few milligrams of the sulfide samples (1-2 mg) were dispersed in few mL (1-2 mL) of n-hexane by ultrasonication for 15 minutes and a drop of the dispersion was placed on a carbon coated copper grid using capillary tube and allowed to dry in air at room temperature. The grids were then introduced to the microscope column, which was evacuated to less than 1 $\times$ 10^{-6} Torr. Specimens were enlarged using thin photographic paper. The sizes of the particles visible in the photograph were measured manually and averaged. This characterization technique was used for the identification of the active sulfide phases on the support.

3.4.5   Temperature programmed desorption (TPD):

The acidity of the catalysts was measured by the temperature-programmed desorption (TPD) of NH_3 (AutoChem 2910, Micromeritics, USA). The standard procedure for the TPD measurements involved the activation of the sample in flowing He at 873 K (1 h), cooling to 323 K, adsorbing NH_3 from a He-NH_3 (10 %) mixture, removing the physisorbed NH_3 in a flow of He at 323K for 30 min, and finally carrying out the TPD experiment by raising the temperature of the catalyst in a programmed manner (10 K/min). The areas under the TPD curves were converted into meq. NH_3 desorbed per gram of catalyst based on injection of known volumes of the He-NH_3 mixture under similar conditions. A lower temperature of 673 K was used in the case of the sulfide catalysts to avoid stripping of S. Confirmation that a lower drying temperature did not have any effect on the desorption profiles (of sulfide catalysts) was obtained by an experiment conducted by drying (MCM-41 based catalyst) at 773 K. The TPD profiles from both experiments were similar. Sulfidation of the samples was done using n-heptane containing 1 wt% of S as DMDS at 553K. The sulfided sample was flushed in a flow of N_2 at 553K to remove adsorbed hydrocarbons and S-compounds before cooling to RT (in N_2).

3.4.6   Temperature programmed reduction (TPR):

To evaluate the reduction profiles of the catalyst Temperature Programmed Reduction (TPR) was carried out. TPR profiles were obtained on a commercial apparatus (Micromeritics TPD/TPR 2900) interfaced with a computer. Prior to the measurements, the catalyst was dried in a TPR cell at 873 K for 2 h in a stream of He to remove water and adsorbed impurities. The TPR profiles were then obtained by passing a 10% H_2/Ar flow (60 mL min^{-1}) through the sample at temperatures from 303 to 873 K. The temperature was increased at the rate of 15 °C min^{-1} and the amount of H_2 consumed was determined with a

Thermal Conductivity Detector (TCD). A cooling trap was placed between the sample and the TCD to retain the water produced during the reduction process.

3.4.7   Raman Spectroscopy:

Characterization of Mo loaded oxidic catalysts was carried out using Raman spectroscopy. This spectroscopic technique provides insight into structure of oxides, their crystallinity, the co-ordination of metal oxide sites and in some cases the spatial distribution of the phases when used in microprobe mode. As the frequencies of metal-oxygen vibrations in a lattice are typically found to range between few hundred to 1000 cm^{-1}, infrared analysis can not be used. Raman spectra were recorded on a Horiba JY Lab RAM HR 800 Raman spectrometer coupled with a microscope in reflectance mode with 633 nm excitation laser source and a spectral resolution of 0.3 cm^{-1}.

3.5 Experimental set up:
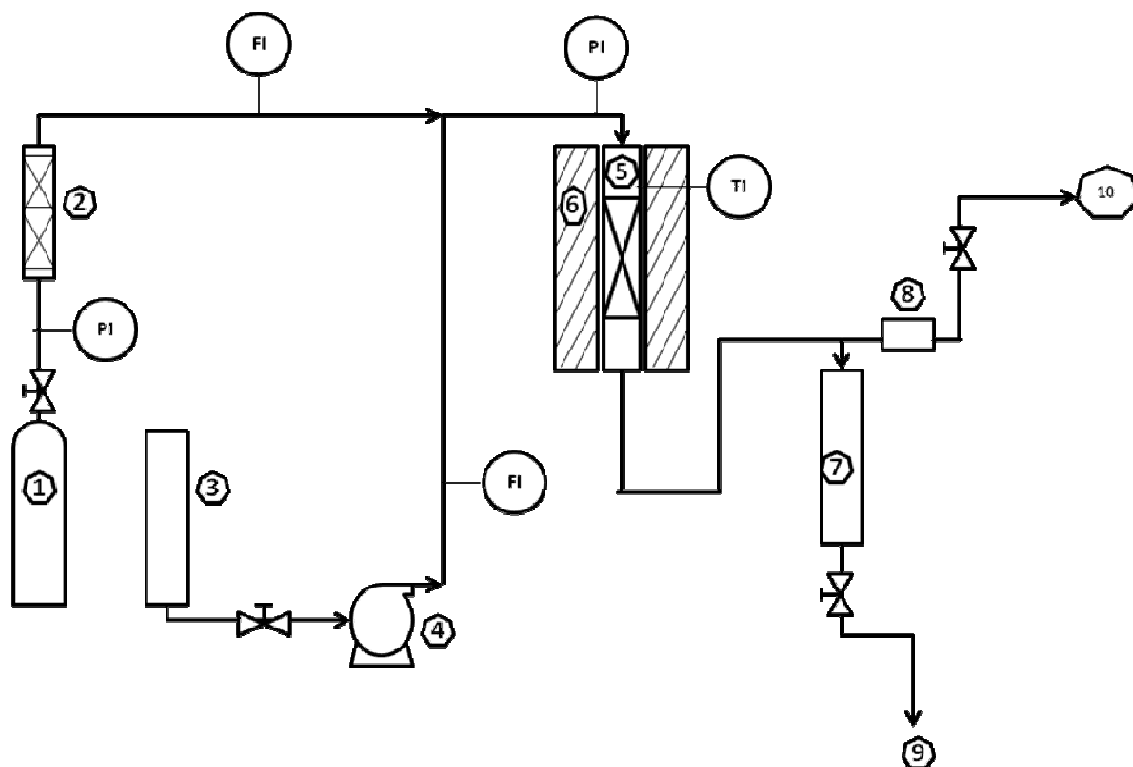
Figure 3.1: Schematic diagram of Experimental set up

1. Hydrogen Cylinder, 2. Molecular Sieve trap, 3. Feed, 4. HPLC Pump, 5. High pressure fixed bed microreactor, 6. Furnace (Heater), 7. Gas Liquid Separator, 8. BPR, 9. Product collection (For GC or UV-Vis analysis), 10. Vent

PI – Pressure Indicator, FI – Flow Indicator, TI – Temperature Indicator

The experimental set up for hydrotreating reactions (HDN, HDS and HDM) is shown in Figure 3.1. The reactions were carried out in high pressure fixed bed micro-reactor. The feed for the reaction was pumped using a high pressure liquid chromatography (HPLC) pump. Hydrogen flow desired for the reaction for constant H_2/feed ratio was controlled by mass

flow controller. The reactor was pressurized using a back pressure regulator to the desired pressure. Products were collected from the gas-liquid separator outlet and were analyzed.

3.6 Reaction Procedure

3.6.1 Hydrodenitrogenation Reaction Procedure

Hydrodenitrogenation (HDN) of quinoline (Q) and 1,2,3,4-tetrahydroquinoline (1THQ) was studied using the two catalysts (NiO (4 %)-MoO$_3$ (15 %) supported on γ-Al$_2$O$_3$, SBA-15) in a high-pressure fixed-bed continuous-flow stainless steel reactor (i.d = 8mm) operated in the down-flow mode. About 3 g of catalyst (1-2 mm size) was loaded and dried *in situ* in N$_2$ at 553 K for 4 h. The catalyst was then pre-sulfided at 553 K using 1 wt% dimethyl disulfide (DMDS; 6800 ppm sulphur) in decalin at 30 bar pressure (WHSV (h^{-1}) = 1; H$_2$/N (mole/atom) = 48; H$_2$/liquid feed (v/v) = 400 STP) for 6h. Subsequently, the reactor temperature, pressure and H$_2$ flow rate were adjusted to the required value and the reaction was started by injecting the feed. The feed was 5 wt% N-compound (Q or 1THQ) in decalin, corresponding to feed N contents of 5420 ppm for Q and 5260 ppm for 1THQ. The feed was spiked with 1wt% DMDS (6800 ppm S) to prevent loss of S from the catalyst and consequent deactivation. The conditions of the HDN experiments were as follows: temperature, 553 – 613 K; WHSV, 1.0 h^{-1}; pressure, 50 bar and H$_2$/liquid feed (v/v) = 400 STP. Usually, product analysis was carried out after attainment of a steady state (12h) after each temperature change.

3.6.2 Cumene cracking

Cumene cracking activity of the sulfided catalysts was carried out in the temperature range 623 - 723K to find out their acidity in the sulfided state at temperature conditions

43

similar to that used for the HDN reactions. About 1g of catalyst was pre-sulfided at 553 K using 1 wt% dimethyl disulfide (DMDS; 6800 ppm S) in cumene at atmospheric pressure (WHSV (h^{-1}) = 1; H_2/cumene (v/v) = 400; duration = 6h). The cumene cracking activity was measured by GC analysis of the product collected over a six hour period after completion of the presulfidation step.

3.6.3 Hydrodesulfurization reaction procedure:

Hydrodesulfurization (HDS) of dibenzothiphene (DBT) and 4.6 – dibenzothiophene (4,6-DMDBT) was carried out using two catalysts (NiO (4 %)-MoO_3 (15 %) supported on γ-Al_2O_3, SBA-15) in a high-pressure fixed-bed continuous-flow stainless steel catalytic reactor (i.d = 8mm) operated in the down-flow mode. About 3 g of catalyst (1-2 mm size) was loaded and dried *in situ* in N_2 at 553 K for 4 h. The catalyst was then pre-sulfided at 553 K using 1 wt% dimethyl disulfide (DMDS; 6800 ppm sulphur) in decalin at 30 bar pressure (WHSV (h^{-1}) = 1; H_2/N (mole/atom) = 48; H_2/liquid feed (v/v) = 400 STP) for 6h. Subsequently, the reactor temperature, pressure and H_2 flow rate were adjusted to the required value and the reaction was started by injecting the feed. The feed was mixture of DBT and 4,6 – DMDBT in decalin solvent equivalent to 1000 ppm of sulfur. In this case feed was not spiked with DMDS since the feed already consisted of sulfur compounds. The conditions of the HDS experiments were as follows: temperature, 553 – 613 K; WHSV, 1.0 h^{-1}; pressure, 50 bar and H_2/liquid feed (v/v) = 400 STP. Usually, product analysis was carried out after attainment of a steady state (12h) after each temperature change.

3.6.4   Hydrodemetallation reaction procedure:

Hydrodemetallation (HDM) reactions were carried out using 5,10,15,20 – tetraphenyl – *21 H, 23 H* porphine (Ni-TPP) as a model compound. Since this reactant was not soluble in decalin, paraffin oil was used as solvent. The model compound was not soluble at room temperature. Ni-TPP was carefully weighed and care was taken that it is not exposed to atmosphere since this compound has strong tendency of getting oxidiized. This compound was added to paraffin oil in stainless steel autoclave. The autoclave was then purged with nitrogen for 15 minutes and the mixture was allowed to stir at 80 deg C for 1 hr to remove dissolved oxygen. The reaction mixture was then kept at 200 – 220 deg C for the period of 12 hrs. The mixture was then brought to room temperature and filtered using 0.5 μm filter paper. The concentration of the porphyrin in solution was found out from a standard graph of absorption vs. concentration obtained from solutions of the compound in n-hexane. The red coloured porphyrin solution was used as feed for the reaction. The reaction was carried out in high-pressure fixed-bed continuous-flow stainless steel catalytic reactor (i.d = 8mm) operated in the down-flow mode. About 1 g of catalyst was loaded and dried *in situ* in N_2 at 553 K for 4 h. The catalyst was then pre-sulfided at 553 K using 1 wt% dimethyl disulfide (DMDS; 6800 ppm sulphur) in decalin at 30 bar pressure (WHSV (h^{-1}) = 1; H_2/N (mole/atom) = 48; H_2/liquid feed (v/v) = 400 STP) for 6h. Subsequently, the reactor temperature, pressure and H_2 flow rate were adjusted to the required value and the reaction was started by injecting the feed. The conditions of the HDM experiments were as follows: temperature, 553 – 633 K; WHSV, 1.0 h^{-1}; pressure, 50 bar and H_2/liquid feed (v/v) = 400 STP. Usually, product analysis was carried out using UV- Visible spectroscopy after attainment of a steady state (5h) after each temperature change.

3.7 Product analysis

Analysis of the products was carried out by capillary gas chromatography (Mayura Analytical GC - Model 9800; Column: dimethylpolysiloxane (AT-1), 30m x 0.25mm i.d x 0.25 μm film thickness). Identification of the products was carried out by comparison of retention times with standard samples and by GC-MS analysis. Product compositions were estimated from GC areas. The method of gas chromatographic analysis was used for HDN and HDS reaction's product analysis.

Analysis of the products obtained by HDM reaction was carried out by UV-Visible absorption spectroscopy. n-hexane was used as a reference solvent. The products obtained at different temperatures were diluted with n-hexane in 1:5 proportion. The absorption spectra was then recorded. Ni content in the products obtained was found out by comparing the relative peak intensities.

CHAPTER IV

RESULTS AND DISCUSSIONS

Part I. Characterization of catalysts

The results obtained from the characterization studies carried out over the two supports and the oxide and sulfided forms of the catalyst are presented in this chapter.

4.1 X-ray powder diffraction studies
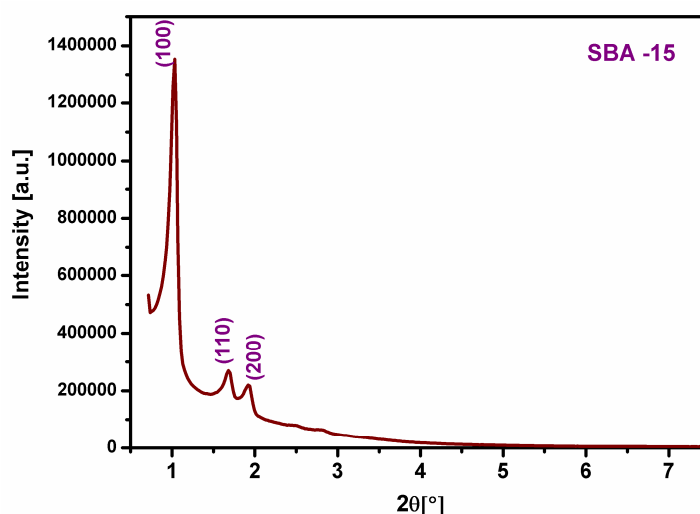
Fig. 4.1. Low angle XRD pattern for calcined SBA-15

The low angle XRD pattern of the SBA-15 is presented in Fig. 4.1. The pattern is typical of those reported for these materials. The a_o value calculated from the d_{hkl} (100) spacing for the above SBA-15 sample is 10.18 nm, which is similar to the values reported by earlier workers [Zhao et al.(1998),Grun et al (1997), Russo et al. (2007)].

The large angle XRD patterns of the oxide forms of the catalysts prepared from alumina and SBA-15 after loading MoO_3 (15 wt%) and NiO (4 wt%) are presented in Fig. 4.2. The patterns reveal the absence of peaks due to the supported oxides in alumina, but peaks attributable to $NiMoO_4$ and MoO_3 are visible in the patterns of the catalysts prepared from the siliceous supports, the lines due to $NiMoO_4$ being very prominent. The patterns suggest that large crystallites of $NiMoO_4$ are present in these oxide catalysts along with much smaller crystallites of MoO_3. The presence of MoO_3 in the catalysts prepared from SBA-15

implies that MoO_3 is poorly dispersed on the siliceous support (SBA-15) compared to alumina.
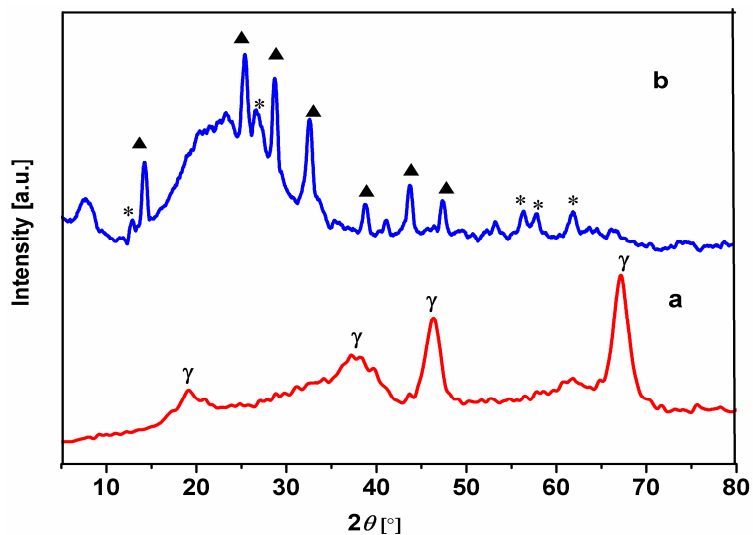
Fig.4.2. XRD patterns of the oxide forms of the catalysts prepared from Al_2O_3 and SBA-15.

(γ – Alumina; * - MoO_3; JCPDS - PCPDFWINv.200 files: γ – Alumina, 29-1486 ; $NiMoO_4$, 33-0948; MoO_3, 76-1003)
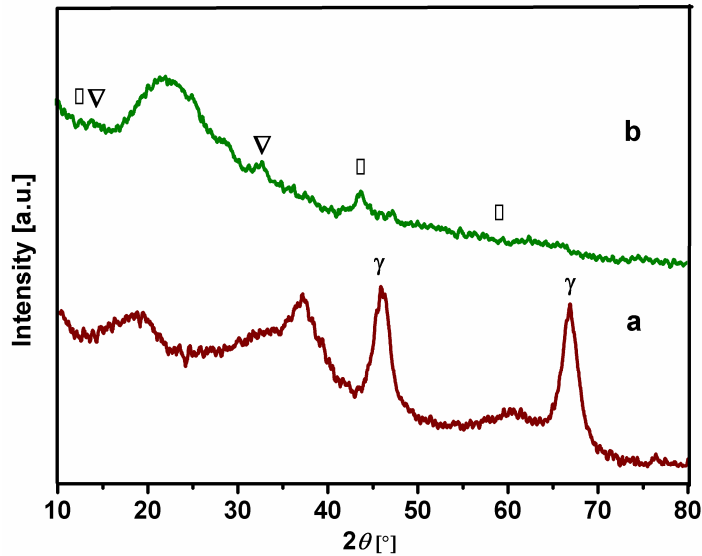
Fig.4.3. XRD patterns of the sulfided forms of the catalysts prepared from Al_2O_3 and SBA-15.

Al_2O_3.(γ – Alumina; ∇- MoS_2; □ - NiS (JCPDS - PCPDFWINv.200 files: γ – Alumina, 29-1486 ; MoS_2, 87-2416; NiS, 89-1495)

The XRD patterns of the sulfided catalysts are presented in Fig. 3.3. The lines due to $NiMoO_4$ and MoO_3 are not seen though weak lines due to NiS are visible in the patterns of the catalysts prepared from SBA-15. Very weak and broad lines attributable to stacked MoS_2 slabs are barely identifiable in these patterns.

4.2 N$_2$-adsorption-desorption studies

Figure 3.4 presents the N_2 adsorption-desorption isotherms and corresponding pore size distribution for SBA-15. A typical type IV adsorption isotherm with a H1 hysteresis loop is observed. The isotherm exhibits a sharp inflection in the p/p_0 range of 0.65 to 0.80 characteristic of capillary condensation within fairly uniform pores. The sharpness of the inflection suggests a very uniform pore-size distribution.
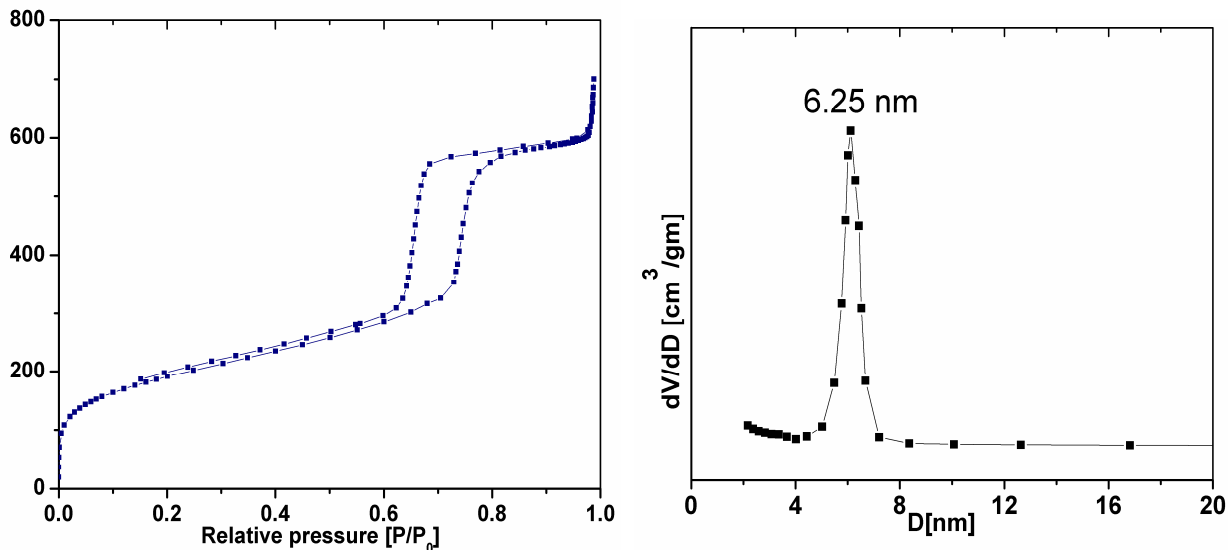
Fig 4.4. N$_2$ adsorption-desorption isotherms of SBA-15 (left) and pore size-distribution obtained by the BJH method from the desorption branch of the isotherm (right).

Surface areas, pore volumes and average pore diameters of the samples obtained by N_2-adsorption are presented in Table 3.1. The average pore diameters of the supports are in the mesopore range (7.2 to 8.3 nm). The surface area of SBA-15 is large (663 m^2/g) compared to that of Al_2O_3 (201 m^2/g) .On loading the active components (NiO, 4 wt% and MoO_3, 15 wt%), the surface areas decrease substantially. Still, the areas of the catalysts containing SBA-15 are nearly double those of Ni-Mo-Al_2O_3. The pore volumes of SBA-15 and Ni-Mo/SBA-15 are 1.06 and 0.61 cm^3/g.

49

Table. 4.1. Surface area, pore volume and acidity of the supports and oxide catalysts

Sample / composition [code]	$S_{BET}{}^a$ (m^2/g)	$S_{Ext.}{}^b$ (m^2/g)	$PV_{total}{}^c$ (cm^3/g)	$PV_{meso}{}^d$ (cm^3/g)	Av. pore size (nm)
Al_2O_3 [AL]	202	192	0.42	0.41	8.3
SBA-15	663	(521)	1.06	0.92	7.2
NiO (4 %)-MoO_3 (15%) /Al_2O_3 [Ni-Mo/AL]	165	152	0.29	0.28	7.1
NiO (4 %) MoO_3 (15%)/ SBA-15 [Ni-Mo/SBA-15]	335	291	0.61	0.59	7.2

^{a}: Surface areas calculated by the BET method; ^{b}: Area obtained after subtracting t-plot micropore area from S_{BET}; ^{c}: N_2 (liq) sorbed at $p/p_o = 0.99$; Pore volume after subtracting t-plot micropore volume from PV_{total}.

4.3 Temperature Programmed Desorption studies

Fig. 4.5. Temperature programmed adsorption profiles of NH₃ from A: supports, B: oxide catalysts and C: sulphide catalysts.

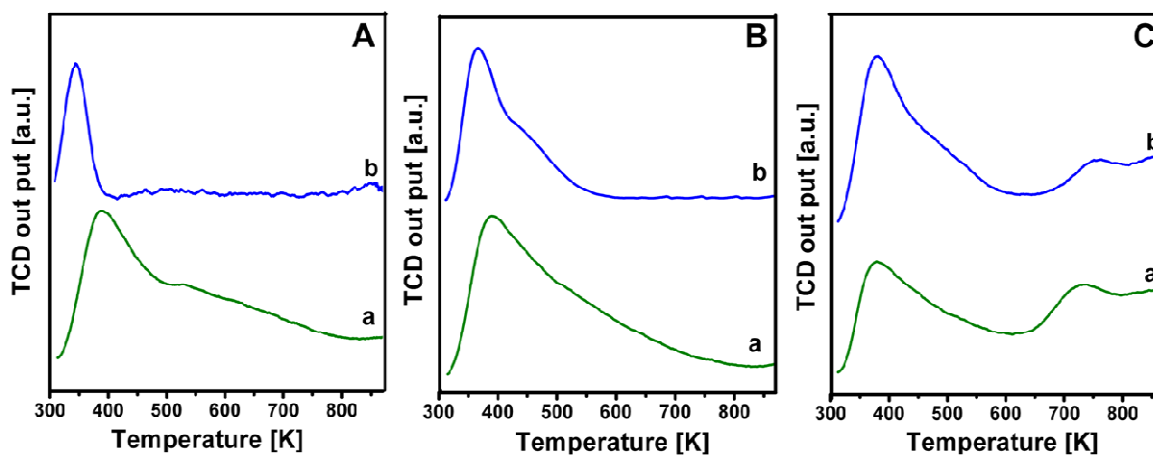The TPD profiles of the supports and the catalysts in the oxide and sulphide states are presented, respectively, in Fig. 4.5. A , B and C. The acidity values obtained from the TPD profiles of both the supports and catalysts are presented in Table 3.2. While the total acidity

of the sample is given by the area under the TPD curves, an idea of the distribution of acidity in the sample may be obtained from the amount of NH_3 desorbed at different temperatures, the temperature -

Table 4.2. Acidity characteristics of supports and catalysts

Support	Acidity (mmol/g)[a]					
	Catalyst					
	Support		oxide form[d]		sulphided[e]	
	> 650 K[b]	Total[c]	> 650 K[b]	Total[c]	> 650 K[b]	Total[c]
Alumina	0.07	0.80	0.06	0.71	0.12	0.65
SBA-15	-	0.30	-	0.82	0.11	0.81

[a]: NH_3 desorbed per g of sample; [b]: NH_3 desorbed beyond 650 K; [c]: NH_3 desorbed based on total area under the TPD curve; [d]: MoO_3(15wt%) and NiO(4%) loaded on the supports; [e]: after sulfidation of the oxide forms.

- of desorption being directly related to the strength of the acid sites. A break-up of the amount of NH_3 desorbed below and beyond 673 K is also presented in Table 3.2. This break-up is expected to reveal the amount of weak and strong acidity in the catalysts. It is found that SBA-15 has the least amount of total acidity and all of the NH_3 desorbs below 400 K revealing the presence of only weak acid sites in this material. In the case of the other supports, the TPD curves are broader suggesting the presence of a wider distribution of acidity, alumina exhibiting the broadest distribution of acid sites. SBA-15 being pure a SiO_2 form is not expected to possess strong acidity, only surface –OH groups that are very weakly acidic. However, Brønsted acidity is created when Al^{3+} ions are introduced in a SiO_2 matrix, even though alumina itself is believed to possess only acidity of the Lewis type [Segawa et al. (1982), Chen et al. (1992)]. The TPD results cannot reveal the nature of the acid sites (Lewis or Brønsted), though the amount of acidity and distribution of acid strength can be estimated

from the results. The acidity calculated from the TPD profiles of both the supports and catalysts are presented in Table 4.2. Generally, it is seen that acidity increases when the oxides (MoO_3 and NiO) are impregnated on SBA-15 (Table 4.2). Apparently, new acid sites are created on the SiO_2 surface when MoO_3 (with NiO) is loaded on it. However, the decrease in acidity noticed in the case of alumina after loading of the oxides is difficult to explain. It is probably due to the MoO_3 covering and sterically blocking some of the acid sites present on the alumina surface. It is also probably due to the dissolution of some of the surface area and consequently the destruction of the acid sites by the high pH of the impregnating solution.

On sulfidation, the acidity of the oxide catalysts decreases slightly. Interestingly, significant desorption of NH_3 is found to take place beyond 673 K from the sulfided catalysts (Fig. 4.5 C), the desorption amount being more than that from the supports and oxide catalysts (Table 4.2). The results suggest the creation of new strong acid sites on sulfidation. These sites are presumably the CUS (coordinatively unsaturated sites) formed on MoS_2. The creation of strong acidity of the Lewis type in sulfided MoO_3/Al_2O_3 has already been reported by earlier workers [Ratnasamy and Knözinger *et al.,*1978, Ratnasamy *et al* ,1980].

4.4 Cumene Cracking

The TPD studies used by us measure the acidity characteristics of the catalysts in the oxide state and may not necessarily represent the acidity of the sulfided catalysts at operating conditions. It was therefore decided to evaluate the acidity of the sulfided catalysts in the temperature range of 623 to 723 K using the model reaction, cumene cracking. The cumene cracking activities of the sulfided catalysts are presented in Fig. 4.6. Even though the cracking activity of the catalysts increases with temperature, it is still very small for Al_2O_3 and SBA-

15 even at 723 K. The negligible cracking activity of the Al_2O_3 and SBA-15 based catalysts is due to the absence of Brønsted acidity in the samples.
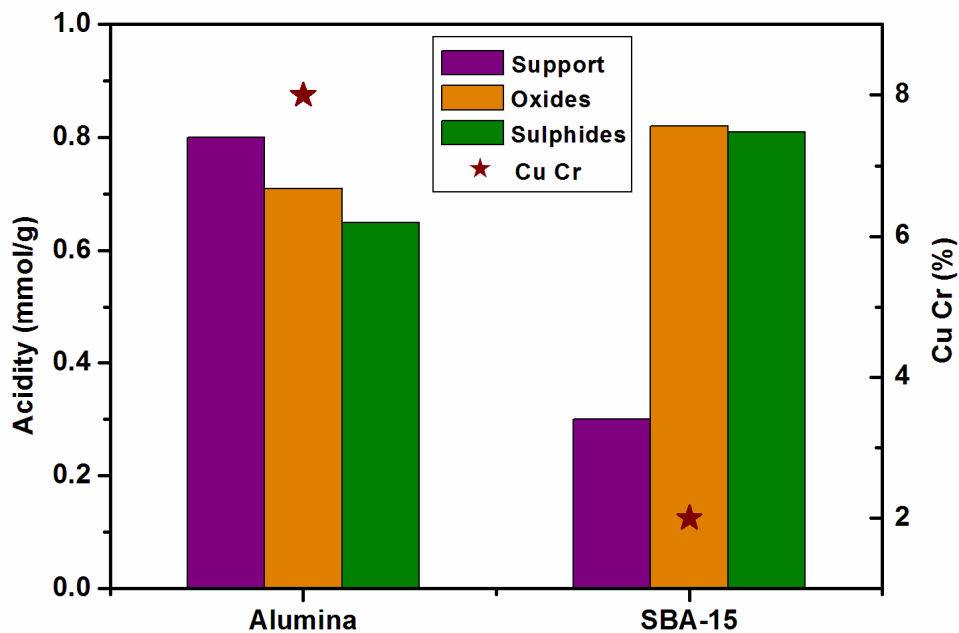

Fig 4.6. Cumene cracking activity of sulfided catalysts Ni-Mo/Alumina and Ni-Mo/SBA-15 (1 st bar : support, 2 nd bar : oxides, 3 rd bar : sulfides

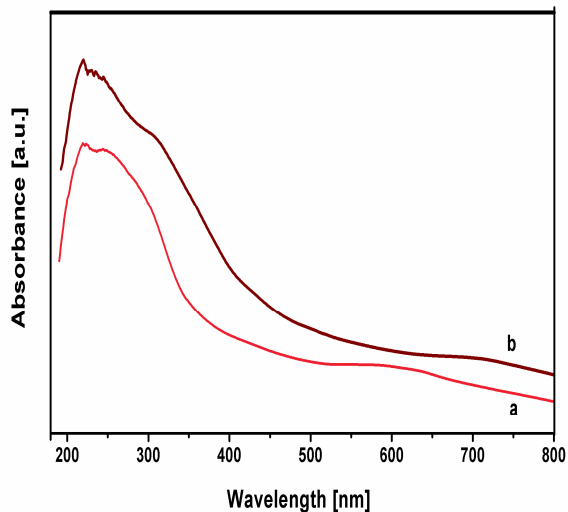## 4.5 UV-Vis. Spectroscopic studies

Fig. 4.7. UV-Vis. spectra of the oxide catalysts; a. Ni-Mo-Al₂O₃ and b. Ni-Mo-SBA-15.

53

The UV-Vis. spectra of the catalysts in the oxide state are presented in Fig. 4.7. Broad absorption bands (from about 200 to 350 - 450 nm) are exhibited by the catalysts, the bands being broader in the case of the siliceous support SBA-15. However, specific humps can be identified in the broad spectra. These are found at about 240, 315, 360, 600 and 700 nm. The band at about 240 nm has been attributed to isolated Mo^{6+} in both T_d and O_h coordination and the one at 315 nm is due to bulk Mo^{6+} in O_h coordination [Williams et al., 1991].The band at about ~315 nm is more prominent in the case of SBA-15, revealing the formation of larger amounts of bulk MoO_3 over this support. The weak bands at 360, 700 nm are attributed to Ni^{2+}(Oh) species and the one at 600 nm noticed in the case of Ni-Mo/alumina is due to Ni^{2+}(Td) from spinel-like phase [Houlla et al., 1980].

4.6 Raman Spectroscopic studies
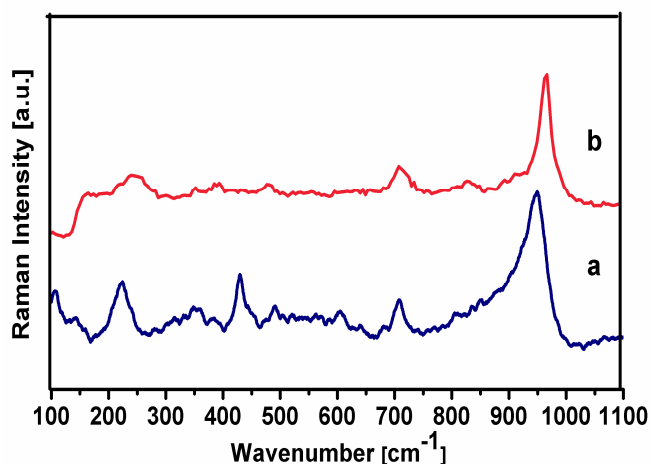
Fig. 4.8. Raman spectra of the oxide samples: a. Ni-Mo-Al$_2$O$_3$ and b. Ni-Mo-SBA-15

The Raman spectra of the catalysts are presented in Fig. 4.8. Examining the spectra, it is found that a band at ~ 710 cm^{-1} is exhibited by both the Ni-Mo-catalysts. This band is attributed to $NiMoO_4$. Levya et al. have recorded the spectra of $NiMoO_4$ and reported the presence of Raman bands at 707, 911 and 959 cm^{-1} [Leyva et al.,2008]. Bands at similar positions are clearly seen in the spectra of the catalysts prepared from SBA-15 (Fig. 4.8). However, in the case of Ni-Mo-Al$_2$O$_3$, only the band at ~710 cm^{-1} is clearly seen, the other two bands being overlapped by the broad band centred at around 950 cm^{-1}. In the case of Ni-Mo/SBA-15 a prominent MoO_3 band at ~ 820 cm^{-1} attributable to bulk MoO_3 is visible. This

54

bands due to MoO_3 is absent in the spectra of Ni-Mo/Al_2O_3 suggesting a better dispersion of MoO_3 over the alumina support than over SiO_2 (SBA-15).

4.7 Temperature programmed reduction studies
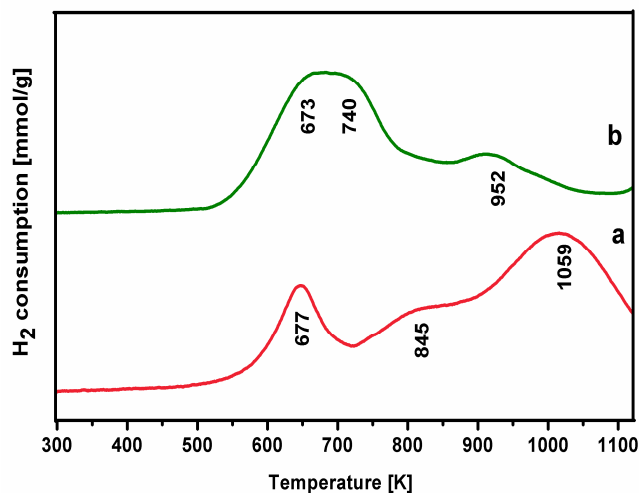
Fig.4.9. Temperature programmed reduction profiles of a. Ni-Mo-Al₂O₃ and b. Ni-Mo-SBA-15

The TPR results obtained over the Ni-Mo catalysts in the temperature range 323 – 1173 K are presented in Fig. 4.9. The reduction profiles are found to be different for the two supports. The reducible ions present in the samples are Mo^{6+} and Ni^{2+}. While Ni^{2+} is expected to undergo reduction to Ni^o, one would expect Mo^{6+} to undergo reduction in two distinct stages: $Mo^{6+} \rightarrow Mo^{4+} \rightarrow Mo^o$, the first stage being the easier one. XRD, UV-Vis. and Raman studies have revealed that Mo and Ni ions are present in different structures (specie) in the catalysts, such as dispersed MoO_3 interacting with the surface, surface polyoxo species, bulk MoO_3 and $NiMoO_4$. In spite of the many species present, the TPR profiles reveal mainly three reduction peaks, though small humps are also seen. In the case of Ni-Mo/Al_2O_3, the TPR peak maxima are found at 677 and 1059 K with a hump at 845 K, the high temperature peak being the major one. This is similar to the results of earlier

55

workers, who have reported two peaks for 12 % MoO_3/Al_2O_3, a minor one at 660 and a major one at 1074 K [Jezlorowski, 1979]. They have attributed the low temperature peak to the partial reduction of amorphous, highly defective, multi-layered Mo-oxides and the high temperature peak to the deep reduction of all Mo-species including highly dispersed $Mo(T_d)$. A similar explanation is also applicable in this case. In general, peak maximum temperatures for the reduction peaks are larger (677 – 1059 K) for Ni-Mo-Al_2O_3 than for Ni-Mo-SBA-15 (673 – 952 K) suggesting a greater difficulty in reducing the Mo-specie when supported on Al_2O_3. This observation implies a weaker interaction of MoO_3 on SBA-15 than on Al_2O_3.

4.8 Transmission Electron Microscopic studies

The transmission electron microscoscopic pictures of the sulfided form of Ni-Mo-SBA-15 at different magnifications are presented in Fig. 4.10. The pictures reveal distinctly the ordered arrangement of the pores in the SBA-15 sample (Fig. 4.9 A & B). Besides, stacked slabs of MoS_2 are also seen in Fig. 4.10 C & D.
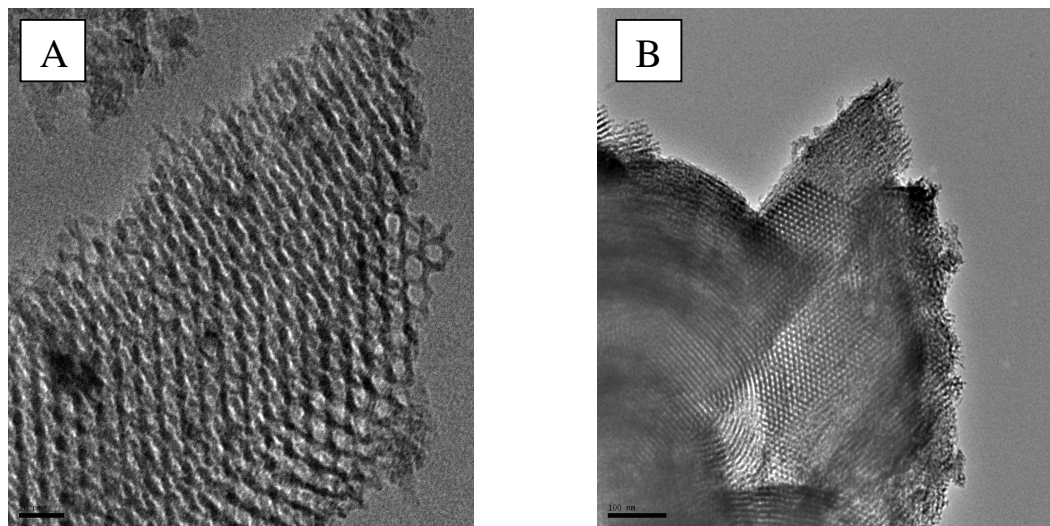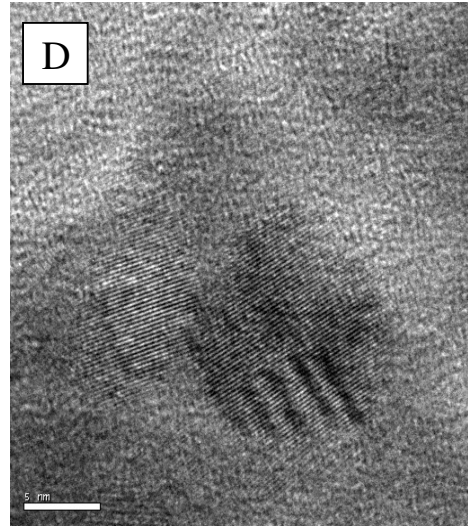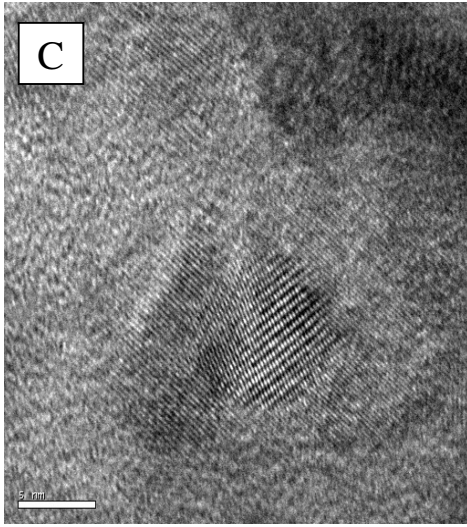
Fig 4.10. Transmission electron micrographs of sulfided Ni-Mo-SBA-15 (A,B,C,D).

CHAPTER IV

# RESULTS AND DISCUSSIONS

Part II. Hydrotreating Reactions

In the earlier chapter (Chapter III), the two different supports, alumina and silica (SBA-15) were found to affect the characteristics (physico-chemical properties) of the oxides supported on them. It is hoped, therefore, that the catalytic activities of the two catalysts made from the two supports will be different. In this chapter, the activity of the two different catalysts, prepared from alumina and SBA-15 (silica) on three important hydrotreating reactions, viz. HDN, HDS and HDM are investigated.

4.9 HYDRODENITROGENATION (HDN)

The studies carried out on the hydrodenitrogenation of quinoline and 1,2,3,4-tetrahydroquinoline over the two catalysts (Ni-Mo/Al$_2$O$_3$ and Ni-Mo/SBA-15) are presented in this section.

The sequence of reactions taking place during the HDN of Q has been identified and the reaction pathways are shown in Scheme 1 [Jian et al 1998]. The different products reported in this work are identifiable in the scheme. The HDN of polycyclic aromatic nitrogen compounds starts by hydrogenation of the nitrogen-containing aromatic ring followed by ring opening elimination to give an aliphatic amine or an arylamine or cyclohexylamine. In the first, the heterocycle in quinoline (Q) is hydrogenated to 1,2,3,4- tetrahydroquinoline (THQ-1) rather than to 5,6,7,8-tetrahydroquinoline (THQ-5) which hydrogenates into decahydroquinoline (DHQ). The former step is a very fast reaction and, under most conditions, equilibrium is reached between Q and THQ-1**.** Thereafter, ring opening of the heterocycle to o-propylaniline (OPA) takes place via the highly reactive *o*-propenylaniline intermediate. In principle, propylaniline should be able to undergo denitrogenation just as aniline does. After hydrogenation of quinoline to give THQ-1 and breaking of the first C–N bond (either by elimination or by substitution and C–N hydrogenolysis), the nitrogen atom in 2-propylaniline (OPA) is attached to a C (sp2) atom rather than to a C (sp3) atom. It might therefore be expected that the HDN of quinoline would take place predominantly via OPA.

The overall network of the HDN of Q (Scheme.1) accounts for most of the observed products. HDN over NiMo/Al-MCM(*x*) has been reported to proceed via o-allyl aniline intermediate formed by a E2 reaction. The C-N bond hydrogenolysis of THQ involving SN2 reaction can be part of the overall mechanism as well (Nelson,1979). Final stage involves the HDN of OPA. Jian *et al.* (Jian et al, 1998) demonstrated that under the conditions employed, the HYD of propylbenzene (PBz) (formed from OPA) to propylcyclohexane (PCH) was inhibited by the intermediate N-compounds present. The direct formation of PBz from OPA would involve the breaking of C-N bonds. It is unlikely that such a reaction can play any role during the HDN.
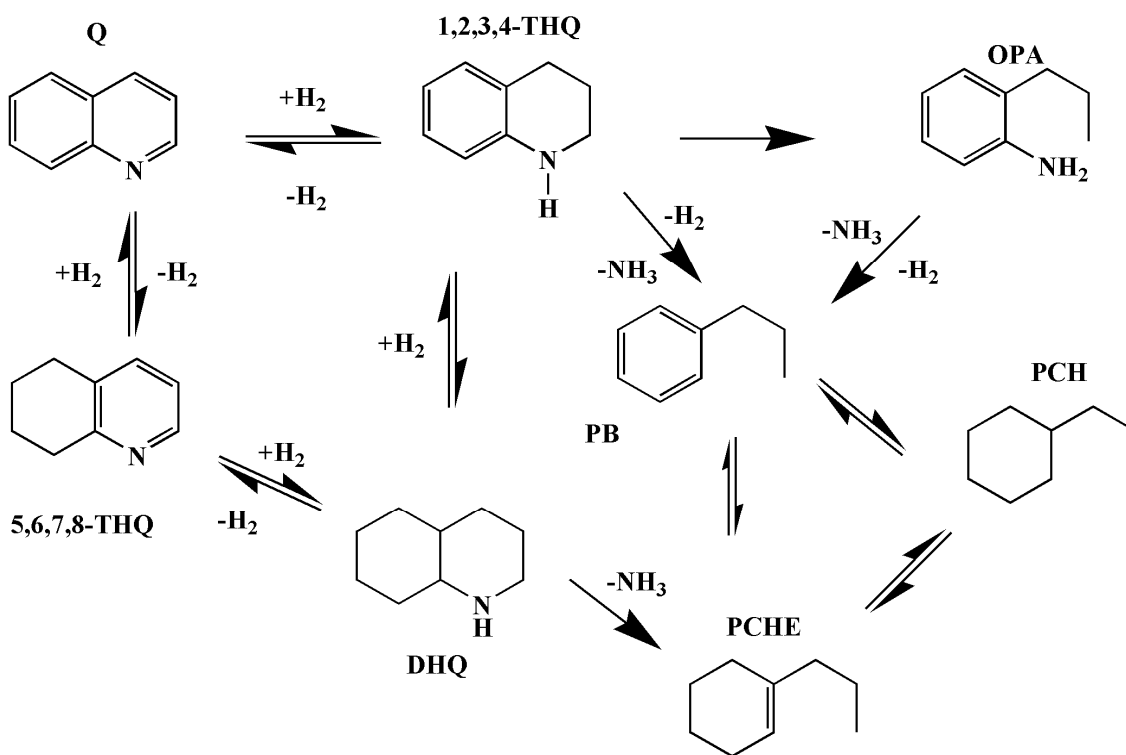
Scheme 1. Reaction network in quinoline hydrodenitrogenation.

4.9.1   HDN of quiniline (Q)

The studies carried out on the HDN of quinoline over the two catalysts, Ni-Mo-Al$_2$O$_3$ and Ni-Mo-SBA-15 are presented in this section.

4.9.1.1 Influence of temperature:

The influence of temperature on the HDN of quinoline over sulfided Ni-Mo/Al$_2$O$_3$ and Ni-Mo/SBA-15 was investigated in the temperature range of 553 - 613 K at 50 bar total pressure, WHSV (h^{-1}) of 1.0 and H$_2$/Q (or 1-THQ) ratio (mole) of 48. The results of these studies are presented in Fig 4.11.

Fig. 4.11. Influence of temperature on conversion of quinoline and product distribution: a) Ni-Mo/Al$_2$O$_3$ and b) Ni-Mo/SBA-15 (Conditions: WHSV (h^{-1}), = 1; press. = 50 bars; H$_2$/liquid feed (v/v) = 400 STP, Feed N-content = 5 wt% ~5420 ppm in decalin).

The conversion is almost 100% for both the catalysts even at 553 K, the lowest temperature of investigation. The major product of the conversion is found to be 1-THQ. The next important one is the end product, n-propyl benzene (PB). The expected intermediates, *o*-propyl aniline (OPA), decahydroquinoline (DHQ) and 5,6,7,8-tetrahydroquinoline (5-THQ) are also found in the product in different amounts. Over Ni-Mo/SBA-15 (the less acidic catalyst), the yield of 1THQ is nearly 100 % at 553 K. This suggests that the transformation

of Q into 1THQ occurs rapidly over the hydrogenation sites present in the catalyst, and the transformation of 1THQ into OPA is slower, probably requiring acid sites. It is noticed that larger amounts of OPA are present in the products from Ni-Mo/Al$_2$O$_3$ than in the products from Ni-Mo/SBA-15. This could be due to the rapid cracking of 1THQ at the –C—N- bond to produce OPA, and the relatively slower conversion of OPA into PB. Over the weakly acidic Ni-Mo/SBA-15 the formation of PB starts only after 593 K, while over Ni-Mo/γ-Al$_2$O$_3$, the formation of PB starts after 553K.

4.9.1.2 Influence of feed-rate:

The reaction profiles and product yields as a function of feed-rate are presented in Fig 4.12. The results reveal that conversion of quinoline is nearly constant (~100%) in the WHSV range investigated. Conversion of 1-THQ increases with the increase in the contact time (1/WHSV) along with the formation of the final product propylbenzene (PB) in the case of both the catalysts. The interesting observations are that the yield of OPA goes through a maximum at the intermediate contact time of 1 h in the case of Ni-Mo/Al$_2$O$_3$, while PCH goes through a maximum in the case of Ni-Mo/SBA-15. These observations could imply different mechanistic pathways for the two catalysts, the HDN taking place mainly via the cracking of 1-THQ in the case of Ni-Mo/Al$_2$O$_3$ and mainly via cracking of DHQ (decahydroquinoline) in the case of Ni-Mo/SBA-15. This conclusion is also supported by the larger amount of DHQ present in the products from Ni-Mo/SBA-15.

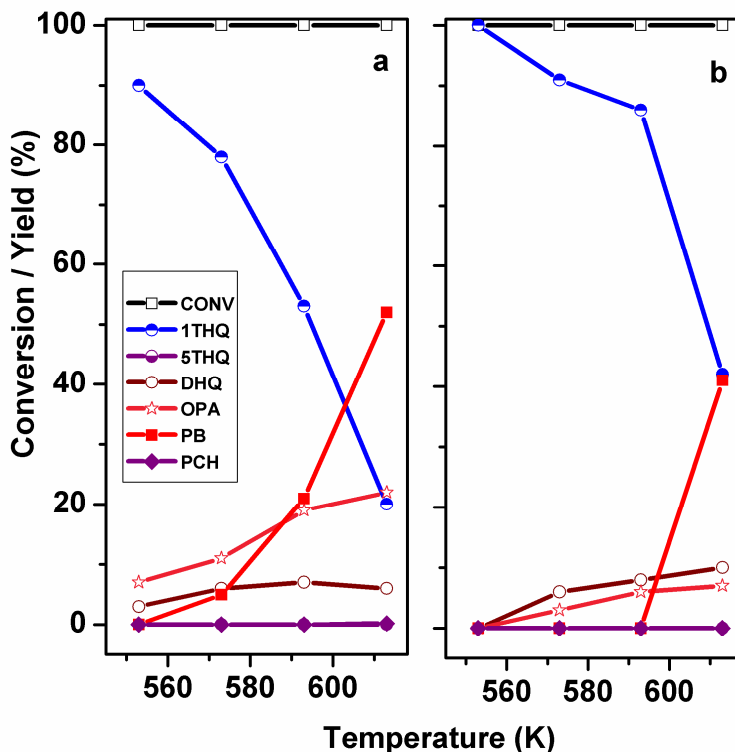**Fig. 4.12. Influence of feed-rate on conversion of quinoline and product distribution: a) Ni-Mo/Al₂O₃ and b) Ni-Mo/SBA-15 (Conditions: Temp. 613 K; press. = 50 bars; H₂/liquid feed (v/v) = 400 STP, Feed N-content = 5 wt% ~5420 ppm in decalin).**

4.9.2   HDN of 1,2,3,4-tetrahydroquinoline (1-THQ)

The studies carried out on the HDN of 1-THQ over the two catalysts, Ni-Mo-O₃ and Ni-Mo-SBA-15 are presented in this section.

4.9.2.1 Influence of temperature:

The influence of temperature on the transformation of 1THQ over the two catalysts is presented in Fig 4.13. The hydrogenated product is DHQ, and the products of cracking are OPA and PB. Minor amounts of 5-THQ, Q and PCH (propylcyclohexane) are also formed over most catalysts. Total conversion and HDN are more over Ni-Mo/Al₂O₃ than over Ni-Mo/SBA-15. Conversion and selectivity for PB increase (as expected) with temperature. In these experiments, PB formation is negligible at 553 K over both the catalysts, but increases rapidly with temperature. The yields of the intermediates, DHQ and OPA go through maxima with temperature in the case of Ni-Mo/Al₂O₃, while only the yield of DHQ goes through a maximum in the case of Ni-Mo/SBA-15. The observed maxima are due to the decomposition

rate overtaking their rate of formation and / or due to equilibrium limitations. The yields of the other products, such as 5THQ, Q and PCH (propylcyclohexane) are small over the two catalysts.

Fig. 4.13. Influence of temperature on conversion of 1-THQ and product distribution: a) Ni-Mo/Al$_2$O$_3$ and b) Ni-Mo/SBA-15 (Conditions: WHSV (h^{-1}), = 1; press. = 50 bars; H$_2$/liquid feed (v/v) = 400 STP, Feed N-content = 5 wt% ~5260 ppm in decalin).

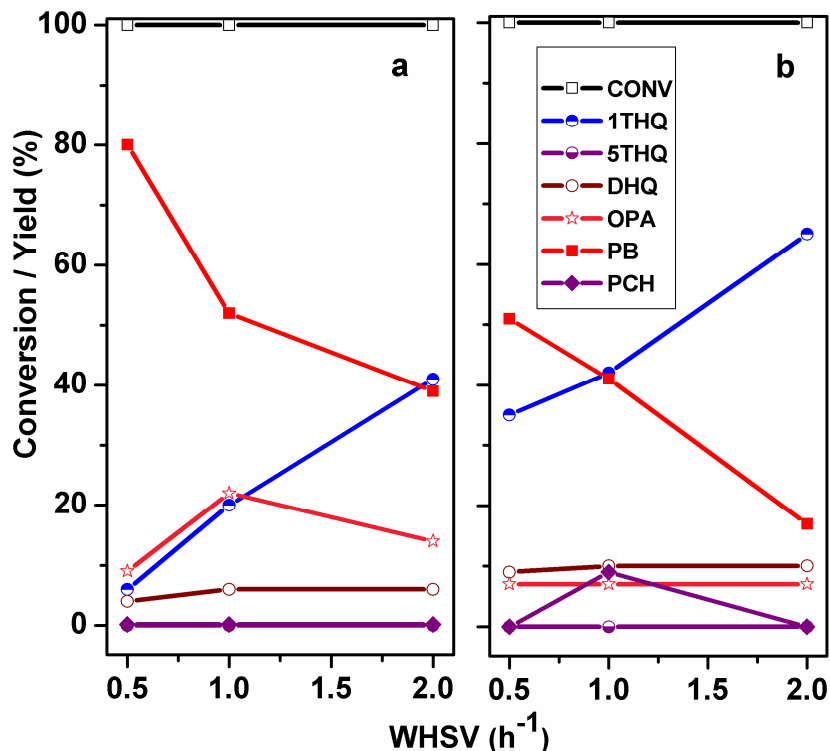**4.9.2.2 Influence of feed-rate:**
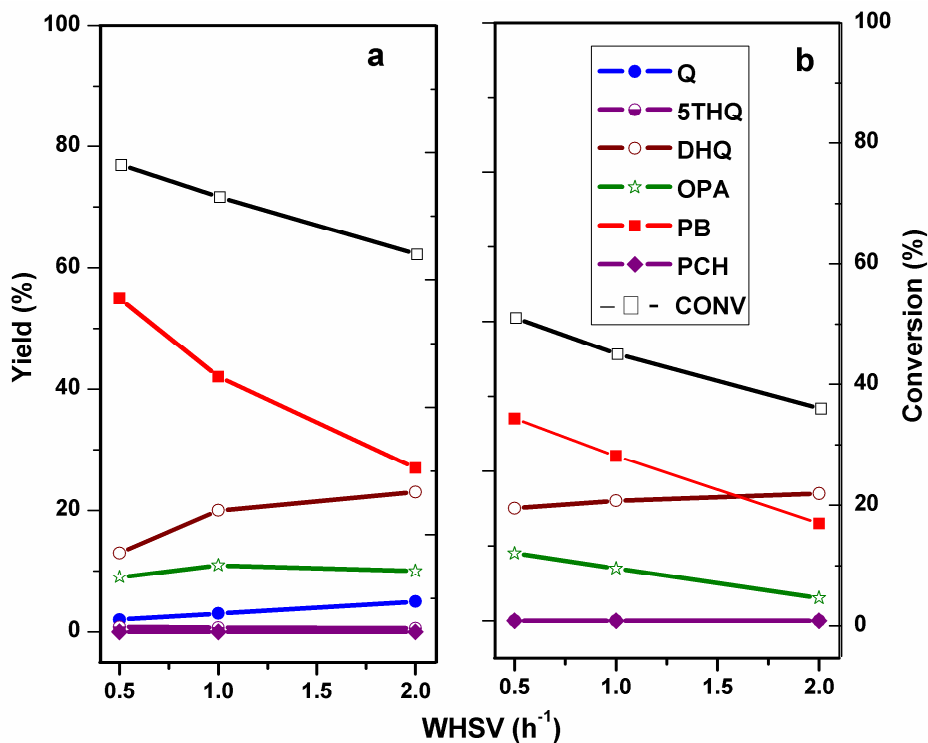
Fig. 4.14. Influence of feed-rate on conversion of 1-THQ and product distribution: a) Ni-Mo/Al$_2$O$_3$ and b) Ni-Mo/SBA-15 (Conditions: Temp. 613 K; press. = 50 bars; H$_2$/liquid feed (v/v) = 400 STP; Feed N-content = 5 wt% ~5260 ppm in decalin).

Both conversion and HDN decrease with increase in feed-rate for both the catalysts. A small amount of Q is formed over the alumina catalyst, presumably by the dehydrogenation of 1-THQ. While the yield of DHQ increases with feed-rate, OPA decreases over Ni-Mo/SBA-15 and is nearly constant over the alumina catalyst. The explanations for these observations are not clear at the moment.

4.10   HYDRODESULPHURIZATION (HDS)

Studies on the hydrodesulfurization of dibenzothiophene and 4,6-dimethyl-dibenzothiophene were carried out over the two catalysts (Ni-Mo/Al$_2$O$_3$ and Ni-Mo/SBA-15) and the results are presented in this section.

The sequence of reactions taking place during the HDS of DBT has been identified and the reaction pathways are shown in Scheme 2. The different products reported in this work are identifiable in the scheme. DBT undergoes desulfurization in the presence of hydrogen via two routes. In route 1, DBT undergoes desulfurization via direct desulfurization which involves cracking or hydrogenolysis of the C-S bond to yield biphenyl as the major product. In route 2, one of the phenyl rings of DBT undergoes either partial or complete hydrogenation to yield tetrahydrodibenzothiophene (THDBT) or hexahydrodibenzothiophene (HHDBT) as the major products. These compounds in turn undergo desulfurization to yield phenylcyclohexane (PCH) as the product. Biphenyl (BP) can also undergo hydrogenation of one of the phenyl rings to yield PCH. PCH in turn undergoes complete hydrogenation to yield bicyclohexyl (BCH) as the product.
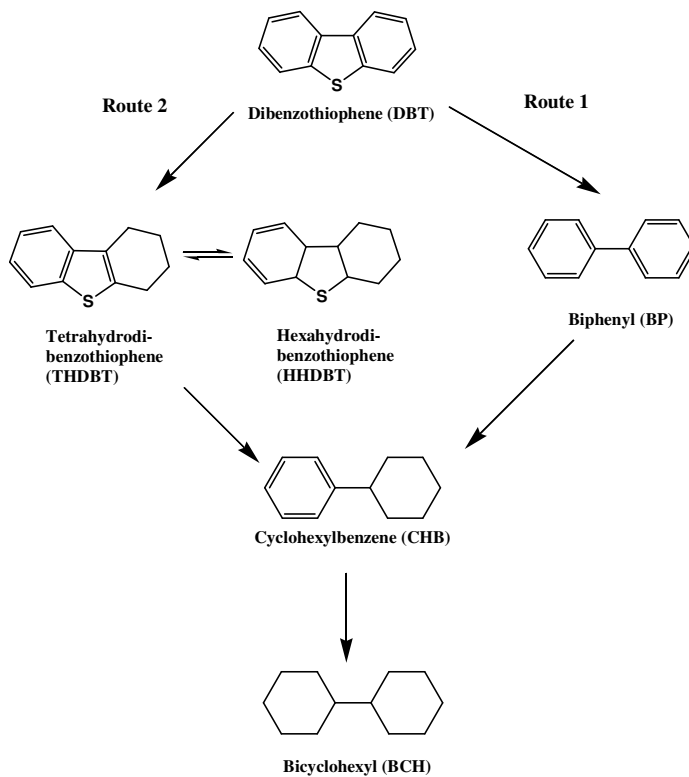
Scheme 2. Reaction network in dibenzothiophene hydrodesulfurization.

65

4.10.1 Hydrodesulfurization of dibenzothiophene (DBT)

The studies carried out on the HDS of DBT over the two catalysts, Ni-Mo-O$_3$ and Ni-Mo-SBA-15 are presented in this section.
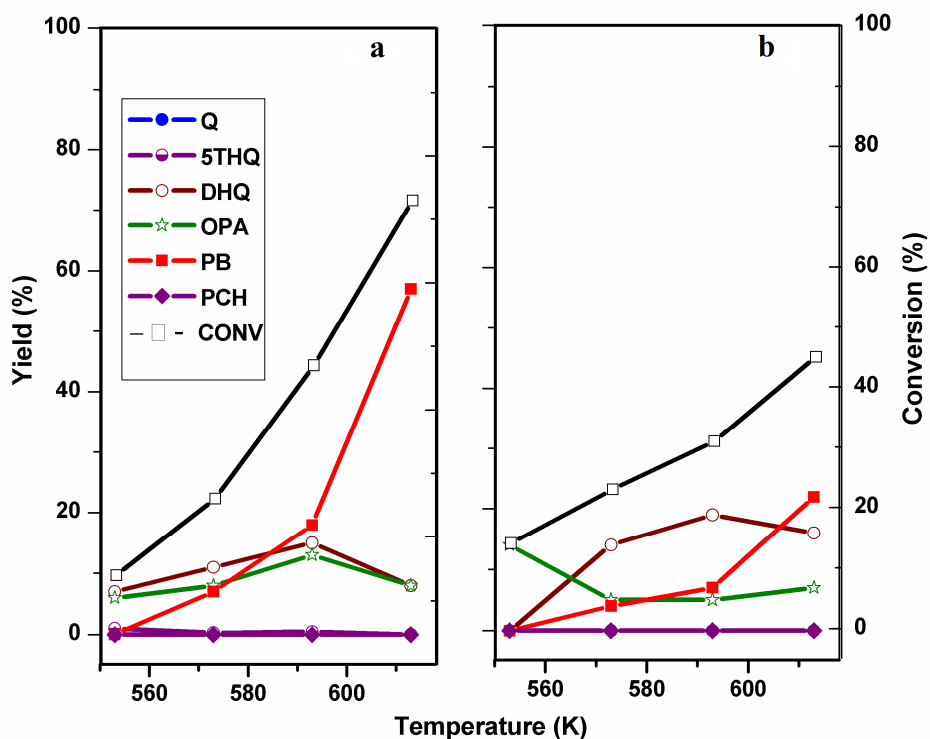
4.10.1.1   Influence of temperature on HDS of DBT:
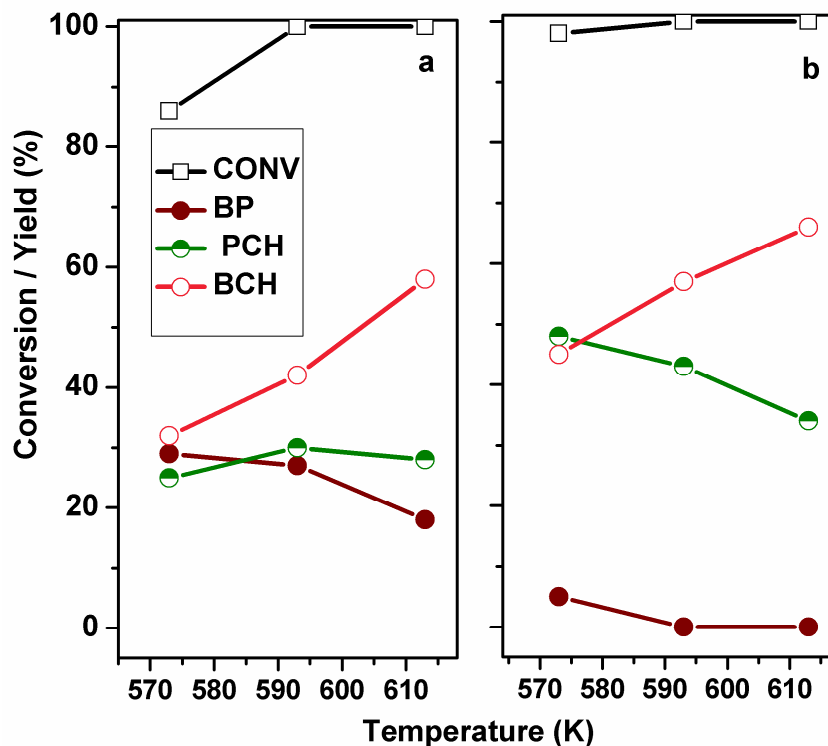
Fig. 4.15. Influence of temperature on conversion of DBT and product distribution: a) Ni-Mo/Al$_2$O$_3$ and b) Ni-Mo/SBA-15 (Conditions: WHSV (h^{-1}), = 1; press. = 50 bars; H$_2$/liquid feed (v/v) = 400 STP; feed S content = 1000 ppm in decalin).

The hydrodesulphurisation of dibenzothiophene has been carried out on sulphided Ni/Mo alumina (a) and SBA-15(b) Fig. 4.15. The effect of temperature was studied from 573- 613K at 50bar pressure with WHSV=1h^{-1}. The conversion is almost for 100% for both alumina and SBA-15. The possible products are biphenyl(BP), phenylcyclohexane (PCH), bicyclohexane(BCH). The yield of hydrogenated product was higher for SBA-15 compared to alumina catalyst.

4.10.2 Hydrodesulfurization of 4,6-dimethyldibenzothiophene (46DMDBT)

The sequence of reactions taking place during the HDS of 4,6 DMDBT has been identified and the reaction pathways are shown in Scheme 3. The different products reported in this work are identifiable in the scheme. 4,6 –DMDBT can undergo desulfurization by various routes. It can undergo direct desulfurization reaction to yield 3,3'-dimethylbiphenyl product. 4,6- DMDBT can also undergo isomerization in which methyl group is shifted to another carbon atom in one of the phenyl rings. This isomerized product undergoes direct desulfurization to either 3,4'-DMBPh or 4,4'-DMBPh based on degree of isomerization. 4,6-DMDBT can also undergo disproportionation reaction in which cracking of one of the methyl group takes place to yield 4-MDBT. This may further undergo disproportionation reaction to yield 3-methylbiphenyl.

Generally 4,6-DMDBT undergoes HDS reaction via hydrogenation route. In this case, one of the phenyl rings may undergo partial or complete hydrogenation to yield hydrogenat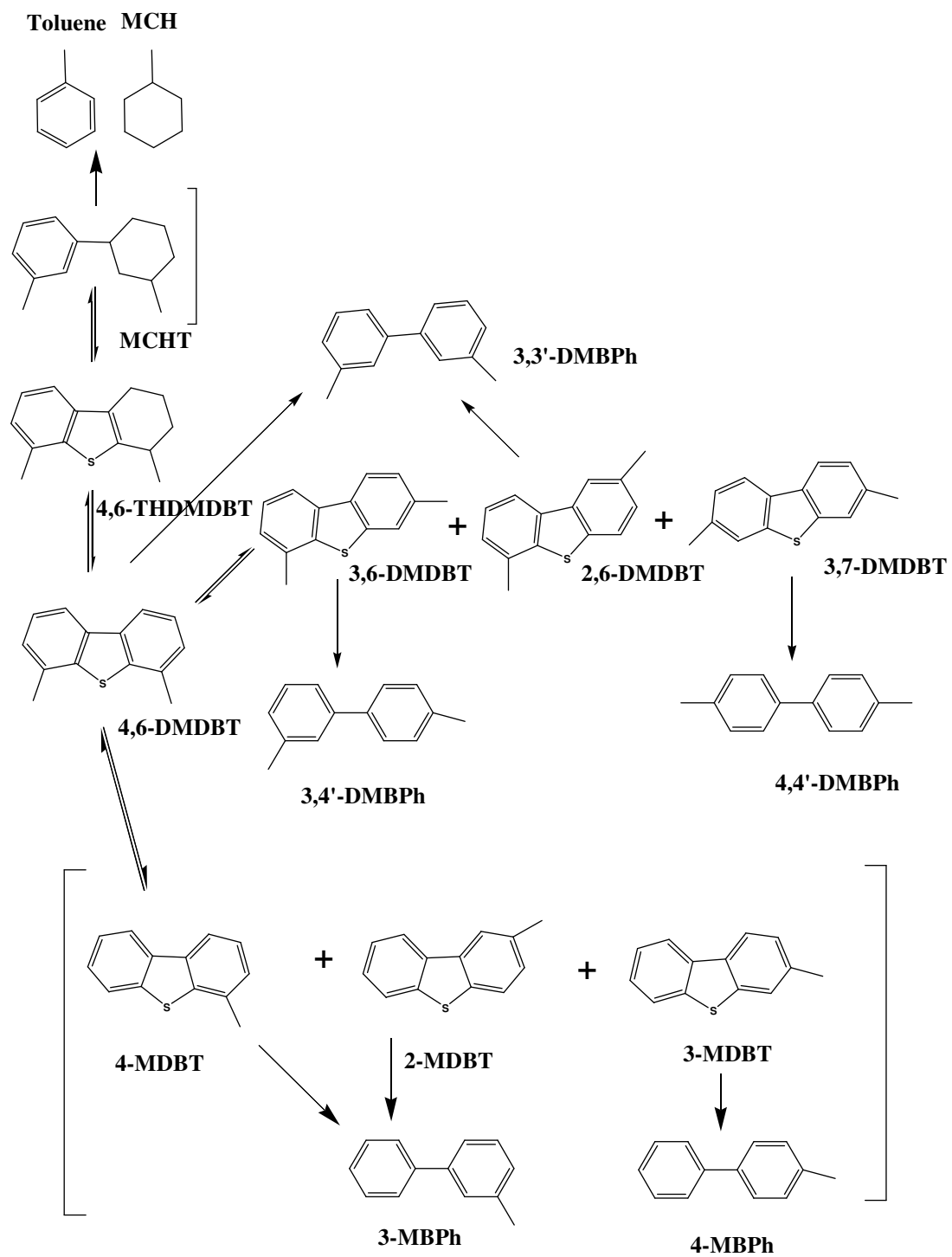ed dimethyldibenzothiophene. This is further followed by C-S bond breaking to yield desulfurized product, methylcyclohexyltoluene (MCHT). This product may further undergo hydrocracking reaction to yield toluene or cyclohexane.

4.10.2.1 Simultaneous hydrodesulphurisation of DBT and 4,6-DMDBT

The sequence of reactions taking place in simultaneous HDS of DBT and 4,6-DMDBT has been identified. Ali et al. (2012) studied simultaneous HDS of DBT and substituted DBT's over phosphorus modified CoMo catalysts supported on alumina. DBT was found to undergo HDS via DDS route while 4,6-DMDBT undergo HDS via hydrogenation route. Thus there was no competition between the HDS of DBT and 4,6-DMDBT. DBT HDS conversion was found to be higher than that of 4,6-DMDBT.

In the present study, the simultaneous HDS of a mixture of DBT (500 ppm) and 4,6-DMDBT (500 ppm) in decalin was investigated over the two catalysts. The influence of temperature and feed rate was investigated. The results of the studies are presented in Figs. 4.6 to 4.9.

Toluene MCH

MCHT

4,6-THDMDBT

3,3'-DMBPh

3,6-DMDBT

2,6-DMDBT

3,7-DMDBT

4,6-DMDBT

3,4'-DMBPh

4,4'-DMBPh

4-MDBT

2-MDBT

3-MDBT

3-MBPh

4-MBPh

Scheme 3. Reaction network in hydrodesulfurization of 4,6-dimethyldibenzothiophene.

4.10.2.1.1 Effect of temperature on simultaneous HDS of DBT and DMDBT

The effect of temperature on HDS of DBT in a mixture of DBT and DMDBT (500 ppm each) are presented in Fig. 4.16 and 4.17. The desulfurization was studied in the temperature range of 573 to 613 K at 50 bar pressure and WHSV of 1 h^{-1}. Under these conditions, the conversion is nearly 100 % for both the S-compounds over both catalysts. The products of the HDS of both DBT and DMDBT are the expected ones.
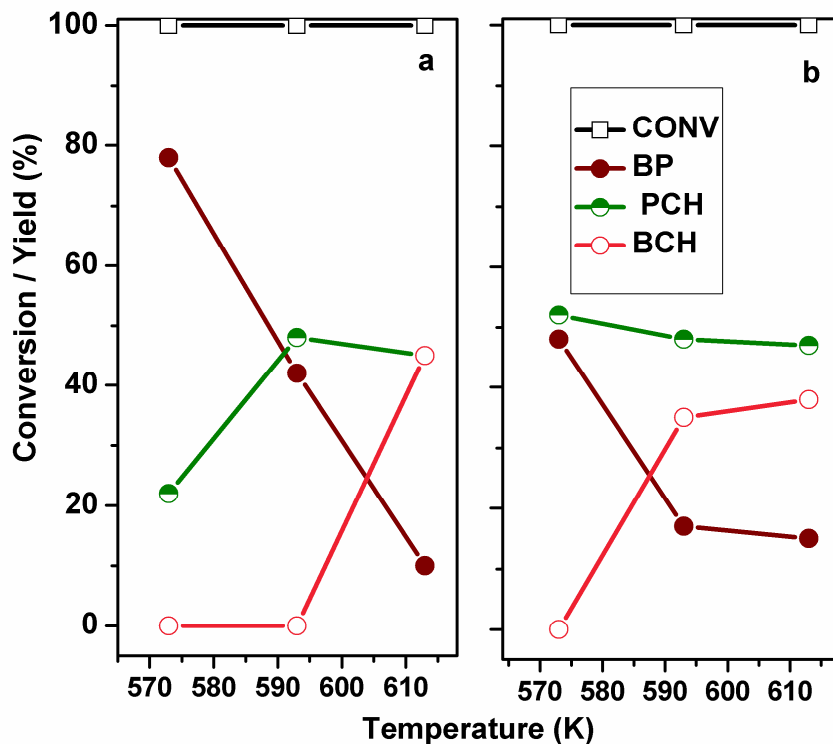
Fig. 4.16. Influence of temperature on conversion of DBT (in a mixture of DBT and 4,6-DMDBT) and product distribution: a) Ni-Mo/Al$_2$O$_3$ and b) Ni-Mo/SBA-15 (Conditions: WHSV (h^{-1}), = 1; press. = 50 bars; H$_2$/liquid feed (v/v) = 400 STP; feed: DBT = 500 ppm; DMDBT = 500 ppm).

Fig. 4.17. Influence of temperature on conversion of DMDBT (in a mixture of DBT and 4,6-DMDBT) and product distribution: a) Ni-Mo/Al₂O₃ and b) Ni-Mo/SBA-15 (Conditions: WHSV (h⁻¹), = 1; press. = 50 bars; H₂/liquid feed (v/v) = 400 STP; feed: DBT = 500 ppm; DMDBT = 500 ppm).

4.10.2.1.2 Effect of feed rate for DBT in presence of DMDBT

The effect of feed-rate on HDS of DBT in a mixture of DBT and DMDBT (500 ppm each) are presented in Fig. 4.18 and 4.19. The desulfurization was studied at 613 K at 50 bar pressure and WHSV of 0.5 to 2 h^{-1}. Under these conditions, the conversion is nearly 100 % for both the S-compounds over both catalysts. The products of the HDS of both DBT and DMDBT are the expected ones (Schemes 2 and 3). The reason for similar reactivity of DBT and 4,6-DMDBT over both the catalysts is the high severity of the reaction conditions (high pressure and low feed rates) making it easy to completely desulfurize even the refractory DMDBT.
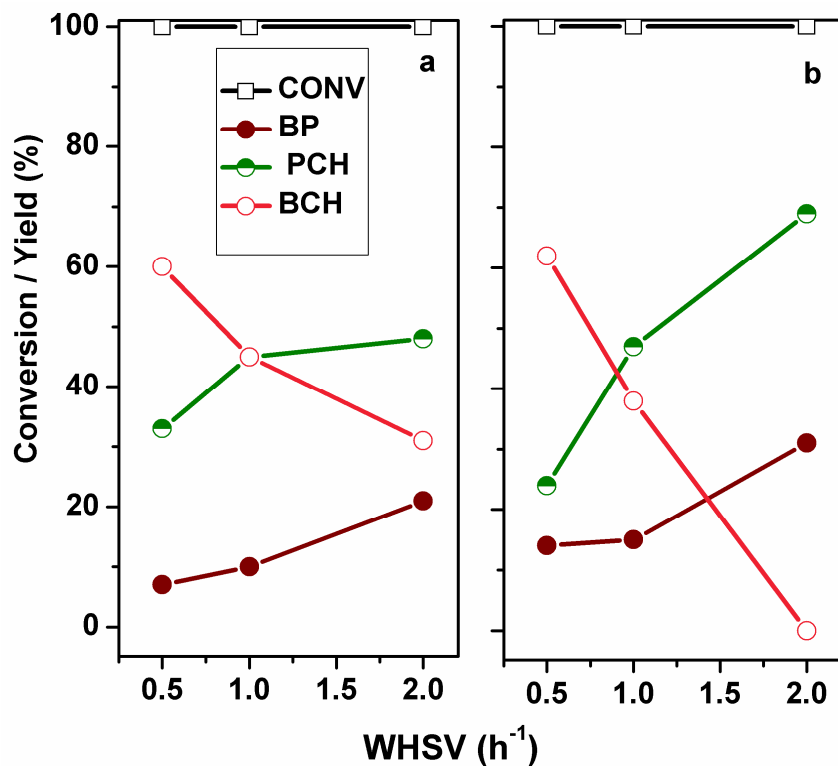
Fig. 4.18. Influence of feed-rate on conversion of DBT (in a mixture of DBT and 4,6-DMDBT) and product distribution: a) Ni-Mo/Al2O3 and b) Ni-Mo/SBA-15 (Conditions: Temp. = 613 K; press. = 50 bars; H2/liquid feed (v/v) = 400 STP; feed: DBT = 500 ppm; DMDBT = 500 ppm)
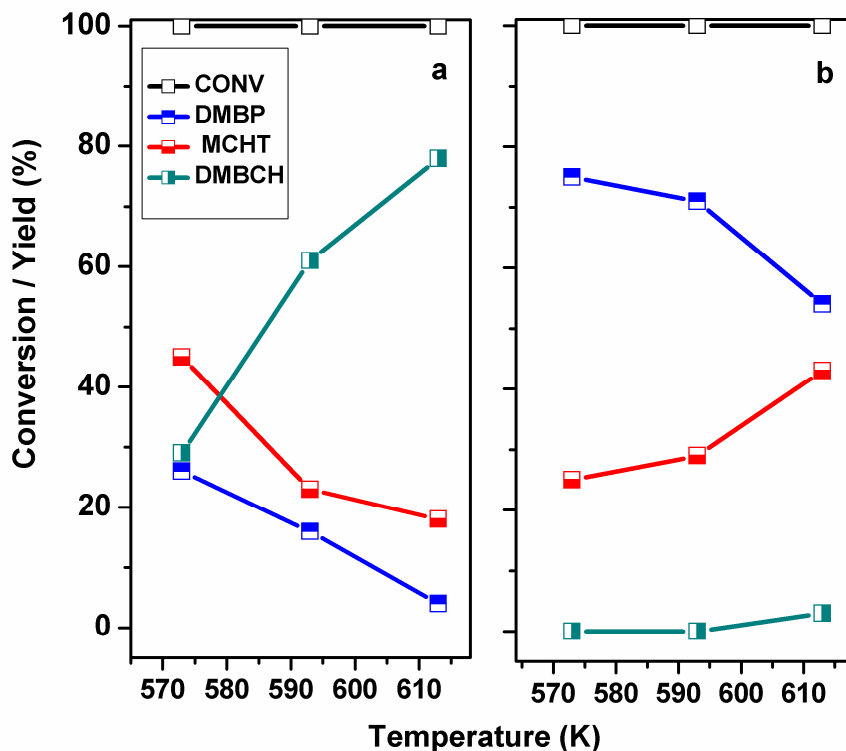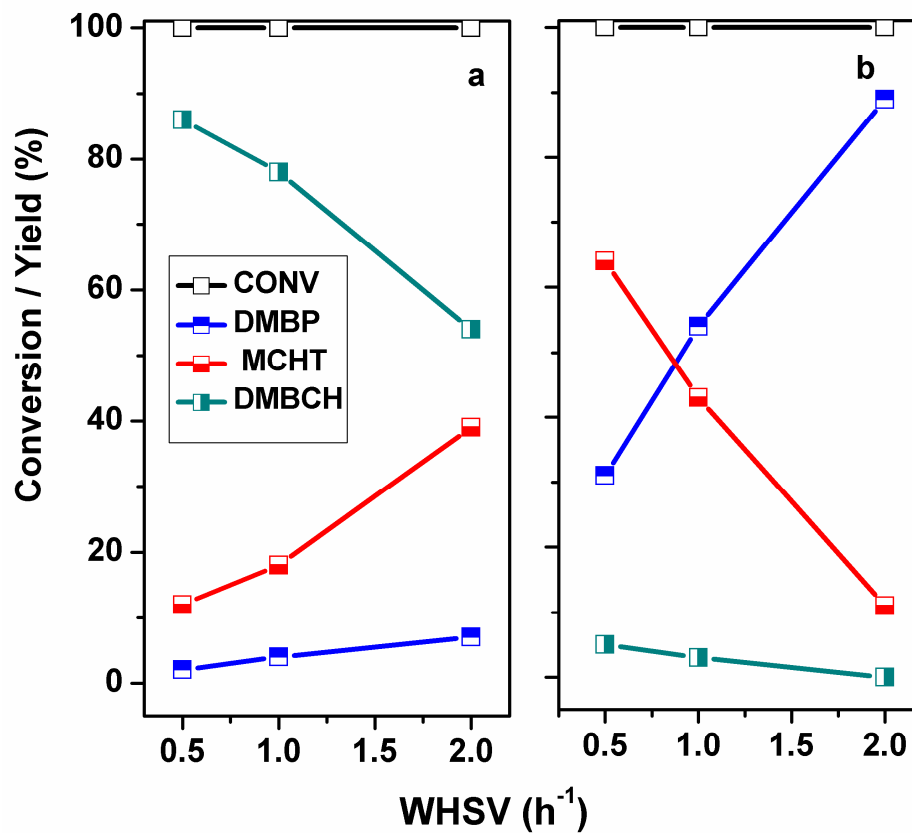
Fig. 4.19. Influence of feed-rate on conversion of DMDBT (in a mixture of DBT and 4,6-DMDBT) and product distribution: a) Ni-Mo/Al2O3 and b) Ni-Mo/SBA-15 (Conditions: Temp. = 613 K; press. = 50 bars; H2/liquid feed (v/v) = 400 STP; feed: DBT = 500 ppm; DMDBT = 500 ppm)

4.11   HYDRODEMETALLATION

The sequence of reactions taking place in the hydrodemetallation of Ni-TPP are shown in the scheme 4. Ni-TPP undergoes the demetallation reaction in the presence of hydrogen through sequential mechanism. Ni-TPP consists of four pyrrole rings connected together with methine bridges. Ni atom lies in the plane of four pyrrole rings. Under high hydrogen pressure, Ni-TPP undergoes hydrogenation of one of the pyrrole rings followed by the hydrogenation of the adjacent pyrrole ring. All the four pyrrole rings may also get completely hydrogenated. After hydrogenation, cracking of Ni-N bond takes place resulting in Nickel sulphide species to be deposited on the catalyst surface.
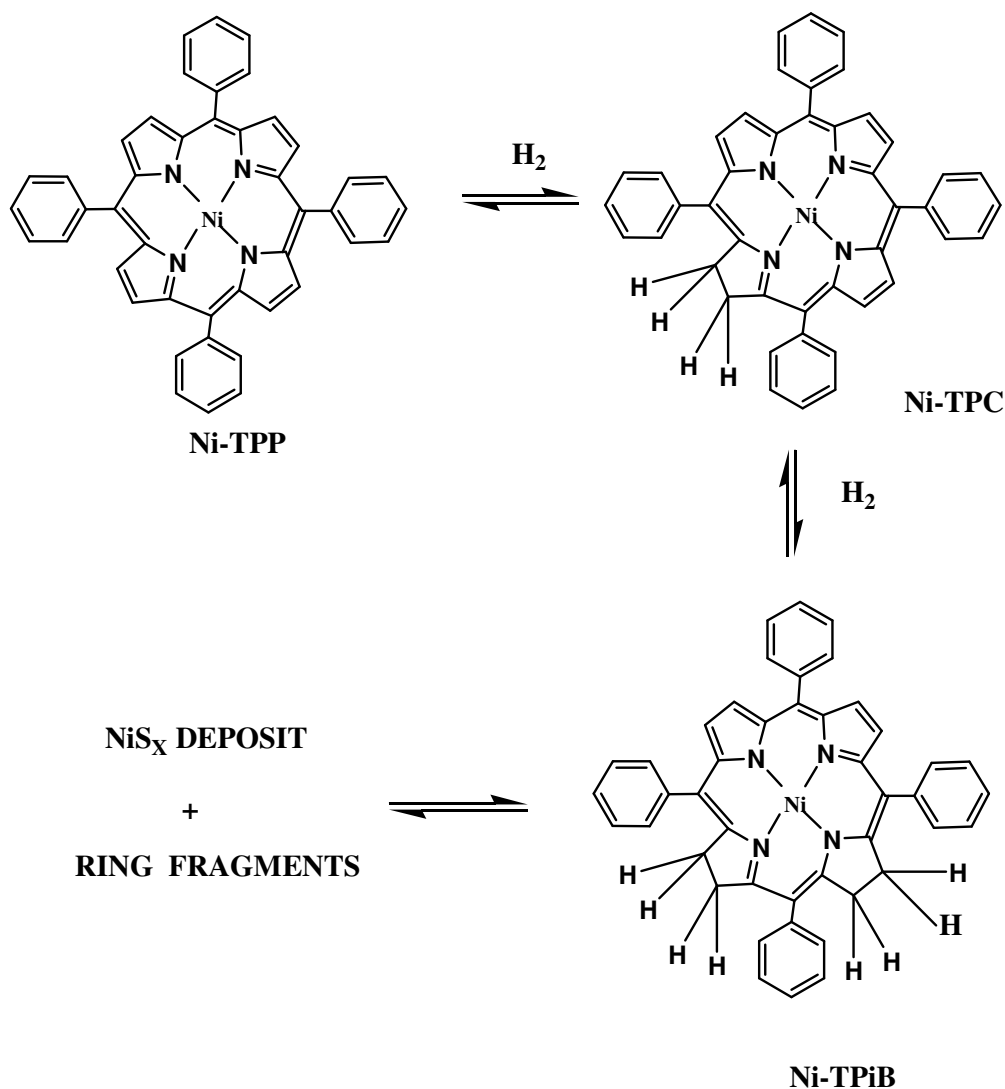
Scheme 4. Reaction network in hydrodemetallation of Ni-teraphenylporphyrin.

4.11.1 Hydrodemetallation of nickel porphyrin

The hydrodemetallation of the nickel porphyrin was carried out in the fixed bed micro reactor. About 3g of the catalyst was loaded and sulphided at 553K, WHSV = 1h-1, press. 30bar for 6h. The reaction was carried out using nickel porphyrin in paraffin oil.

Feed preparation procedure

A solution of Ni-TPP in paraffin oil of relatively high viscosity and boiling point, free of sulfur and nitrogen was used as feed. The solvent (88 g) and the required amount (45.8 mg) of Ni-TPP were warmed up under nitrogen flow from room temperature to 80 ℃. The temperature was held at 80 ℃ for 1 h to eliminate dissolved oxygen in the solvent. The solution was then warmed up to 300 ℃ and maintained at this temperature for 12 h. Then the solution was cooled to room temperature and filtered. The resultant solution contained 27 ppm (weight) of Ni.

UV-Vis spectra

An UV Vis.-absorption intensity vs. concentration plot was made for various concentrations of Ni-TPP in n-hexane. A plot of absorbance vs. different concentrations of Ni-TPP in n-hexane is presented in Fig. 4.20. Using this plot, the concentration of unconverted reactant in the reaction products was calculated. The concentration of the feed Ni-TPP solution was found to be 27ppm.
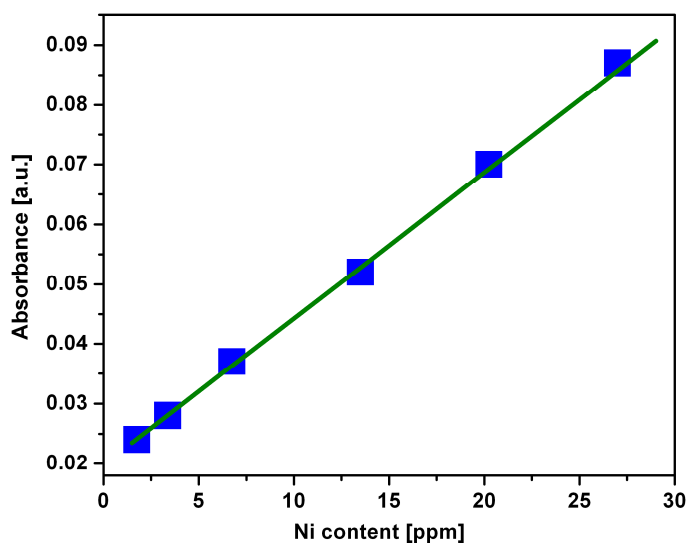
Fig. 4.20. UV Vis.-absorption intensity (525 nm) versus Ni-TPP concentration in n-hexane solutions.

The hydrodemetallation reaction was carried out over the same catalysts investigated in the HDS and HDN reactions, viz. sulfided Ni-Mo/Al$_2$O$_3$ and Ni-Mo/SBA-15. HDM was carried out at different temperatures in the range of 523 to 633 K. HDM activity of the SBA-15 catalyst is found to be more compared to alumina (Fig. 4.21) at all temperatures below 613 K. The conversion is almost 100% even at 553 K over Ni-Mo/SBA-15 while it reaches 100 % only at 613 K in the case of Ni-Mo-/alumina. The reason for the larger HDM activity of Ni-Mo/SBA-15 is its greater accessible surface area and meso-pore volume. The S$_{Ext}$ values are 152 m^2/g and 291 m^2/g, for Ni-Mo/Al$_2$O$_3$ and Ni-Mo/SBA-15 (oxide catalysts), while the PV$_{meso}$ vaues are 0.41 and 0.92 cm^3/g for the two samples in the same order (Table 4. 1).
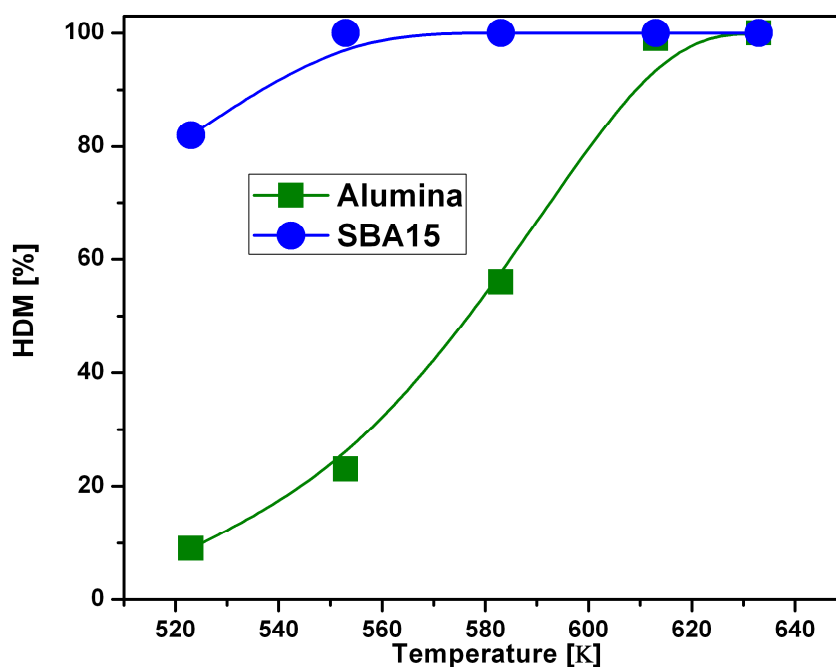
Fig. 4.21. Influence of temperature on HDM of Ni-TPP over Ni-Mo/Al$_2$O$_3$ and Ni-Mo/SBA-15 (Conditions: WHSV (h^{-1}) = 1.0 ; press. = 50 bars; H$_2$/liquid feed (v/v) = 400 STP; feed: 27 ppm Ni-TPP in paraffin oil)

4.12   CONCLUSIONS

Comparison of activities:

The activity of the two catalysts in the three HDT (hydrotreating) reactions investigated (HDS, HDN and HDM) are compared in Fig. 4. 22. Along with the HDT activity of the catalysts, their cumene cracking activities are also presented in the figure. It is noticed that Ni-Mo/Al$_2$O$_3$ is more active than Ni-Mo/SBA-15 for HDN and cumene cracking (CuCr), while the reverse is true for the HDS and HDM reactions. The reasons for these observations are that HDN requires a larger acidity than HDS and HDM reactions and CuCr experiments reveal Ni-Mo/Al$_2$O$_3$ to possess a larger acidity than Ni-Mo/SBA-15.
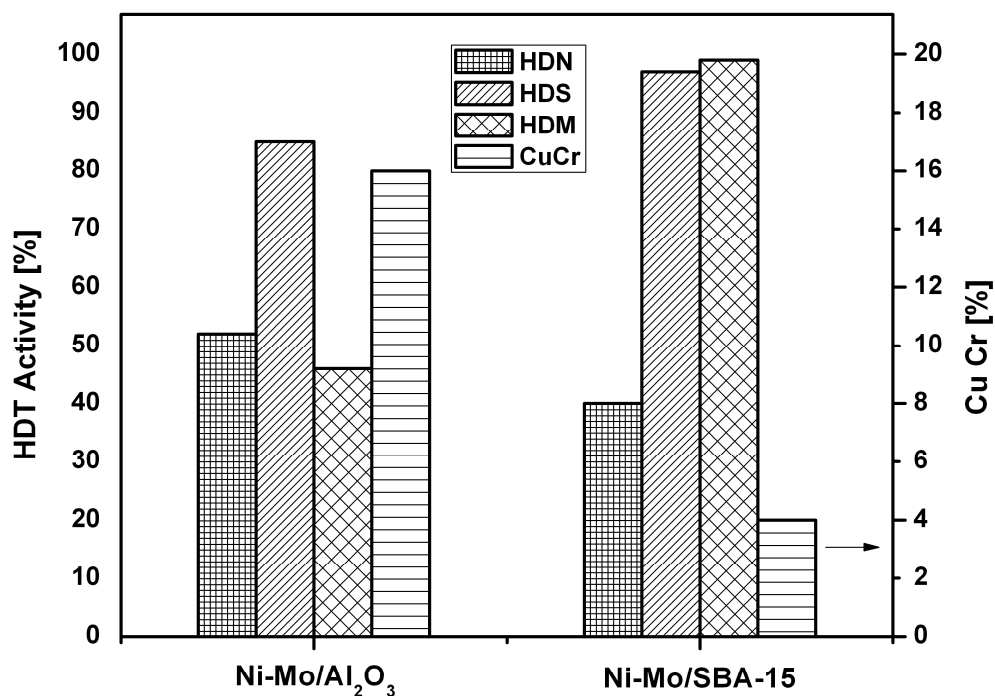
Fig. 4.22. Comparison of activity of sulphided Ni-Mo/Al$_2$O$_3$ and Ni-Mo/SBA-15 in HDS, HDN, HDM and CuCr reactions. (Conditions for HDN: WHSV (h^{-1}) = 1.0 ; press. = 50 bars; H$_2$/liquid feed (v/v) = 400 STP; feed N-content: 5420 ppm in decalin, T = 613 K, Conditions for HDS: WHSV (h^{-1}) = 1.0 ; press. = 50 bars; H$_2$/liquid feed (v/v) = 400 STP; feed S-content: 1000 ppm in decalin, T= 573 K, Conditions for HDM: WHSV (h^{-1}) = 1.0 ; press. = 50 bars; H$_2$/liquid feed (v/v) = 400 STP; feed Ni-content: 27 ppm in paraffin oil, T = 573 K, Conditions for Cumene Cracking : 723 K)

CHAPTER V

SUMMARY AND CONCLUSIONS

Hydrotreating reactions namely hydrodenitrogenation (HDN), hydrodesulfurization (HDS) and hydrodemetallation (HDM) were carried out over in-situ sulfided $NiO\text{-}MoO_3$ supported on γ-alumina and SBA-15. The reactions were carried out using model compounds to understand the mechanism of the reactions. Quinoline (Q) and 1,2,3,4-tetrahydroquinoline (1-THQ) were used as model compounds for HDN reaction. Dibenzothiophene (DBT) and methyl substituted dibenzothiophene (4,6-DMDBT) were used as model compounds for HDS reaction while HDM reaction was carried out using nickel tetraphenylporphyrin (Ni-TPP) compound.

Characterization of the supports was carried out using X-ray powder diffraction (XRD) which suggested that the SBA-15 mesoporous material to be of good quality. XRD characterization was also carried out for the oxide and sulfide catalysts. $NiMoO_4$ and bulk MoO_3 specie were found to be present in the oxide form of Ni-Mo/SBA-15. These species were found in much smaller amounts in Ni-Mo/Al_2O_3. In case of the sulfided catalysts, MoS_2 species were not detected in the alumina catalyst though weak lines corresponding to MoS_2 were visible in the pattern of the SBA-15 catalyst. Analysis of the textural properties of supports and metal oxide supported catalysts was carried out using N_2 adsorption. The average pore diameters of all the supports were found to be in the mesoporous range. Surface area of SBA-15 was found to be higher than γ-alumina. On loading of the metals, surface areas were found to be reduced; however, the pore volume and surface area of the (metal oxides) supported SBA-15 catalyst were nearly double that of the γ-alumina catalyst. Acidity characterization of the supports and oxide catalysts was carried out by NH_3 TPD. SBA-15 was much less acidic compared to γ-alumina, which showed comparatively broad distribution of acid strengths. On loading metal oxides, acidity was found to increase in the case of SBA-15 and not in the case of alumina. UV-visible spectroscopic characterization of oxide catalysts were carried out for co-ordination of metals. SBA-15 showed large amounts of bulk MoO_3 over the supports. Raman spectroscopic characterization was carried out for metal oxide supported catalysts. The studies revealed MoO_3 to be better dispersed on γ-Al_2O_3 compared to SBA-15. Temperature programmed reduction studies were carried out for finding out reduction profiles. Reduction of bulk Mo-species present in the case of SBA-15

was found to be much easier than the well dispersed species present in on the surface of γ-Al_2O_3. TEM images of the SBA-15 support revealed hexagonal pore structure and also the presence of MoS_2 phases on the catalyst.

After systematic characterization, the reactions were carried out in a high pressure fixed bed microreactor in down-flow mode. Effect of temperature was studied on HDN of Quinoline (Q) and 1,2,34-tetrahydroquinoline (1-THQ) at a hydrogen pressure of 50 bar, WHSV of 1 h^{-1} and H_2/N-compound ratio of 48:1 mole. Conversion of quinoline was observed to be 100 % on both the catalysts even at lower temperatures. Yield of 1-THQ was higher in Ni-Mo/SBA-15 compared to Ni-Mo/Al_2O_3, this may be due to rapid hydrogenation of Q. However yield of o-propyl aniline (OPA) was higher in the case of Ni-Mo/Al_2O_3 compared to Ni-Mo/SBA-15. This may be due to rapid cracking of C-N bond in 1-THQ to form OPA and its relatively slower conversion into PB. HDN activity could be determined from the amount of PB formed. Ni-Mo/SBA-15 did not show HDN activity at lower temperatures, though activity increased at higher temperatures. Ni-Mo/Al_2O_3 showed a higher activity compared to Ni-Mo/SBA-15 at all temperatures (553 to 613 K). Investigation of the effect of feed rate (WHSV (h^{-1}) in the range 0.5 – 2.0) revealed that HDN activity decreased rapidly with increasing WHSV. Yields of OPA and propyl cyclohexane (PCH), respectively, were found to be maximum at WHSV = 1 h^{-1} over Ni-Mo/Al_2O_3 and Ni-Mo/SBA-15. This implies that HDN occurs through different mechanistic pathways over the two catalysts.

HDS of dibenzothiophene (equivalent to 1000 ppm sulphur in decalin base) was carried over both the catalysts. Ni-Mo/SBA-15 was found to give higher HDS activity at lower temperatures compared to Ni-Mo/Al_2O_3. At higher temperatures, both catalysts showed 100 % catalytic activity. As per figure 2.3 in this thesis, it can be seen that hydrogenation of DBT is slower compared to direct desulfurization reaction. Presence of more biphenyl indicates that reaction proceeds via direct desulfurization. At higher temperatures, yield of the hydrogenated products was higher in Ni-Mo/SBA-15 catalysts compared to Ni-Mo/Al_2O_3 catalysts. This study was followed by simultaneous HDS of DBT and DMDBT (which has been carried out by very few researchers) each equivalent to 500 ppm of sulphur. DBT conversion was higher (100 %) at lower temperature compared to when DBT alone was used as feed (85 % over Ni-Mo/Al_2O_3 and 97 % over Ni-Mo/SBA-15). Further yield of biphenyl was much higher compared to that in HDS of DBT alone. With increase in temperature, yields of hydrogenation products were found to increase. However the yield of propyl

cyclohexane was much lower, this may due to inhibition of hydrogenation in the presence of DMDBT. In the case of DMDBT-HDS, the major products were dimethyl bicyclohexyl (DMBCH), MCHT (Methylcyclohexyl toluene) and dimethyl biphenyl (DMBP). The presence of dimethyl biphenyl in the products suggests that DMDBT undergoes HDS via DDS route. Ni-Mo/SBA-15 shows higher yields of DMBP compared to Ni-Mo/Al$_2$O$_3$. However, the HYD route was found to be dominating over DDS route in the case of Ni-Mo/Al$_2$O$_3$. Effect of feed rate was also studied for HDS of DBT and simultaneous HDS of DBT and DMDBT. For simultaneous HDS of DBT and DMDBT, the yield of bicyclohexyl (BCH) drastically reduced indicating slower hydrogenation of PCH to BCH at shorter contact times. In the case of DMDBT, HDS by DDS route was dominating compared to HDS by HYD route.

Ni-Mo/Al$_2$O$_3$ and Ni-Mo/SBA-15 were also tested for the hydrodemetallation (HDM) of nickel tetraphenyl porphyrin. The conversion was larger over Ni-Mo/SBA-15 compared to Ni-Mo/Al$_2$O$_3$ at lower temperatures (553 to 613 K). Ni-TPP hydrodemetallation reaction generally goes through hydrogenation of pyrrole rings followed by hydrogenolysis of Ni-N bond. Higher conversion or higher activity of Ni-Mo/SBA-15 may be due to larger accessible area and pore volume compared to alumina.

REFERENCES

Agrawal R., Wei J., 'Hydrodemetalation of Nickel and Vanadium Porphyrins', *Ind. Eng. Chem. Process Des. Dev.,***23** (1984)505-514.

Ahuja S.P., Derrien M.L., Page L. and Jean F., 'Activity and selectivity of hydrotreating catalysts', Ind. Eng. Chem. Pro. Res. Dev., Vol.**9**, No.3,(1970)272-281.

Ancheyta J., Rana M. S., Furimsky E., 'Hydroprocessing of Heavy Petroleum Feeds : Tutorial', *Catal. Today*, **109** (2005) 3-15.

Ancheyta-Juarez J., Maity S.K., Betancourt-Rivera G., Centeno-Nolasco G., Rayo-Mayoral P., Gomez-Perez Ma.T., 'Comparison of different Ni-Mo /alumina catalysts on hydrodemetallization of Maya Crude Oil', *Applied Catalysis A: General*, **216** (2001) 195–208.

Bej S.K., Maity S.K., Turaga U.T., 'Search for an Efficient 4,6-DMDBT Hydrodesulfurization Catalyst: A Review of Recent Studies', *Energy & Fuels*, **18** (2004) 1227 -1237.

Bonne R.L.C, van Steenderen P., van Langeveld A.D., and Mouljin J.A., 'Hydrodemetalization Kinetics of Nickel Tetraphenylporphyrin over Mo/Al$_2$0$_3$ Catalysts', *Ind. Eng. Chem. Res.* , **34** (1995) 3801-3807.

Bonne R.L.C, van Steenderen P., Mouljin J.A., 'Hydrogenation of nickel and vanadyl tetraphenylporphyrin in absence of catalyst', *Applied Catalysis A: General,* **206** (2001) 171–181.

Bookman P.M., Kydd R.A., Sarbak Z., Somogwari A., 'Surface acidity and cumene conversion: III. A study of γ-alumina containing fluoride, cobalt, and molybdenum additives: The effect of sulfidation', *J. Catal.* , **106** (1987) 544-548.

Candia R., Clausen B.S., Morup S, Topsoe H., 'On the catalytic significance of a Co-Mo-S phase in Co-MoAl$_2$O$_3$ hydrodesulfurization catalysts: Combined in situ Mössbauer emission spectroscopy and activity studies', *J. Catal.***, 68** (1981) 453.

Chen F.R., Davis J.G., Fripiat J.J., 'Aluminum coordination and Lewis acidity in transition aluminas', *J. Catal.*, **133** (1992) 263-268.

Chen H.J., Massoth F.E., 'Hydrodemetallation of Vanadium and Nickel porphyrins over sulfided CoMo/Al$_2$O$_3$ catalyst', *Ind. Eng. Chem. Res.,* **27** (1988) 1629-1639.

Chen M., Kumata F., Saito T., Komatsu T., Yashima T., 'Preparation and characterization of Mo catalysts over AlMCM-41/γ-Al2O3 extruded support, *Applied Catalysis A: General*, **183** (1999) 199-208.

Craje M.W.J, Louwers S.P.A, de Beer V.H.J, Prins R., van der Kraan A.M., *J. Phys. Chem*, **96** (1992) 5445.

Cullity, B. D. *Elements of X-Ray Diffraction*. Addison-Wesley Publishing Company, Inc., 1978.

Daage M., Chianelli R.R., *J. Catal*, 149 (1994) 414.

de Jong Krijn P., Synthesis of Solid Catalysts, Wiley VCH , 2008.

Eijsbouts S., van Gestel J.N.M., van Veen J.A.R., de Beer V.H.J. and Prins R., 'The effect of phosphate on the hydrodenitrogenation activity and selectivity of alumina-supported sulfided Mo, Ni, and Ni-Mo catalysts', *J. Catal.*, **131** (1991) 412-432

Fahim Mohamed A., Al-Sahhaf Taher A., Elkilani Amal, *Fundamentals of Petroleum Refining*, First Edition, Elsevier B.V.

Farag H., Whitehurst D.D., Sakanishi K., Mochida I., 'Carbon versus alumina as a support for Co±Mo catalysts reactivity towards HDS of dibenzothiophenes and diesel fuel', Catal. Today **50** (1999) 9-17

Fitz C.W. Jr., Rase H.F., 'Effects of phosphorus on nickel-molybdenum hydrodesulphurization/hydrodenitrogenation catalysts of varying metals content', *Ind. Eng. Chem. Pro. Res. Dev.*, Vol.**22**, No.1, (1983) 40-44.

Frost C.M., Jensen H.B., 'Hydrodenitrification of crude shale oil', *Preprints-American Chemical Society*, Division of Petroleum Chemistry, Vol.**18**, No.1, (1973)119-128.

Furimsky E., Massoth F.E., 'Hydrodenitrogenation of Petroleum', *Catalysis Reviews*, **47**(2005)297–489.

Garcia-Lopez A.J, Cuevas R., Ramirez J., Anchetya J., Nares R., 'Hydrodemetallation kinetics of Ni-TPP over Mo/Al2O3-TiO2 catalyst, *Catal. Today,* **107–108** (2005) 545–550

Grün M., Unger K.K. , Matsumoto A., Tsutsumi K., 'Novel pathways for the preparation of mesoporous MCM-41 materials: control of porosity and morphology', *Micropor. Mesopor. Mater.,* **27** (1999) 207-216.

Houalla M., Nag N.K., Sapre A.V., Broderick D.H., Gates B.C., 'Hydrodesulfurization of dibenzothiophene catalyzed by sulfided CoO-MoO3γ-Al2O3: The reaction network', *AIChE Journal,***24** (1978) 1015-1021.

Houalla M., Delmon B., 'Physicochemical characterization and reducibility of nickel oxide supported on a wide range of silica-aluminas', *J. Phys. Chem.,* **84** (1980) 2194-2199.

Hung C.W., Wei J., 'The Kinetics of Porphyrin Hydrodemetallation. 1. Nickel Compounds', *Ind. Eng. Chem. Process Des. Dev.,* **19** (1980) 250-257.

Jian M., Prins R., 'Kinetics of the Hydrodenitrogenation of Decahydroquinoline over NiMo(P)/Al2O3 Catalysts', *Ind.Eng.Chem.Res.*, **37** (1998) 834.

Jian M., Prins R., 'Mechanism of the Hydrodenitrogenation of Quinoline over NiMo(P)/Al2O3 catalysts', *J. Catal.*, **179** (1998) 18.

Jezlorowski H., Knözinger H., 'Raman and ultraviolet spectroscopic characterization of molybdena on alumina catalysts', *J. Phys. Chem.* **83** (1979) 1166-1173.

Jones D.J., Aptel G., Markus Brandhorst., Mélanie Jacquin., **José Jiménez-Jiménez, Antonio Jiménez-López**, (2000), 'Surface area mesoporous titanium phosphate: synthesis and surface acidity determination', *J. Mater. Chem.*, **8** (2000)1957-1963.

Kasztelan, S., des Courieres, T., and Breysse, M., 'Hydrodenitrogenation of petroleum distillates : industrial aspects', *Catal. Today*, **10** (1991) 433.

Kim H., Lee J.J., Moon S.H., 'Hydrodesulfurization of dibenzothiophene compounds using fluorinated NiMo/Al2O3 catalysts', *Applied Catalysis B: Environmental,* **44** (2003) 287–299

Kwak C., Kim M.Y., Choi K., Moon S.H., 'Effect of phosphorus addition on the behavior of CoMoS/Al2O3 catalyst in hydrodesulfurization of dibenzothiophene and 4,6-dimethyldibenzothiophene', *Applied Catalysis A: General,* **185** (1999) 19-27

Kwak C., Lee J.J., Bae J.S., Choi K., Moon S.H., 'Hydrodesulfurization of DBT, 4-MDBT, and 4,6-DMDBT on fluorinated CoMoS/Al2O3 catalysts', *Applied Catalysis A: General*, **200** (2000) 233–242.

Lee V. , Gioia F., 'Effect of hydrogen pressure on catalytic hydrodenitrogenation of quinoline', *Ind. Eng. Chem. Pro. Des. Dev.*, Vol.**25**, No.4 (1986)918-925.

Leyva C., Rana M.S., Ancheyta A.M., 'Surface characterization of Al2O3–SiO2 supported NiMo catalysts: An effect of support composition', *Catal. Today*, **130** (2008) 345-353.

Liu C., Yu Y., Zhao H., 'Hydrodenitrogenation of quinoline over Ni–Mo/Al2O3 catalyst modified with fluorine and phosphorus', *Fuel Proc. Technol,* **86** (2005) 449-460

Machida M., Sakao Y., Ono S., 'Influence of hydrogen partial pressure on hydrodenitrogenation of pyridine, aniline and quinoline', *Applied Catalysis A: General*, **187** (1999) L73–L78

Maity S.K., Anchetya J ., Soberanis L., Alonso F., 'Catalysts for hydroprocessing of Maya heavy crude', *Applied Catal. A : General*, **253**(2003)125-134.

Mushrush, G.W., Beal, E.J., Hardy, D.R., and Hughes, J.M., 'Nitrogen compound distribution in middle distillate fuels derived from petroleum, oil shale, and tar sand sources', *Fuel Proc. Technol.*, 61(1999)197.

Nelson.N., Levy.R.B., 'The organic chemistry of Hydrodenitrogenation', *J.Catal.*, **58** (1979) 485.

Pecoraro T.A. and Chianelli R.R., 'Hydrodesulfurization catalysis by transition metal sulfides', *J. Catal.*, Vol.**67**, No.2, (1981) 430-445.

Prins R., 'Mechanism and kinetics of hydrodenitrogenation' , *Polyhedron* **16**(1997)3235-3246.

Prins R., 'Catalytic hydrodenitrogenation', Adv. Cat., **46** (2001) 399-464.

Prins R., '*Hydrotreating'*, Handbook of Heterogeneous Catalysis , Volume 6, Second Edition, Wiley VCH, 2695-2718.

Ramanathan S., Yu C., Oyama C. and Ted S., 'New catalysts for hydroprocessing: bimetallic oxynitrides . II. Reactivity studies', *J. Catal.*, Vol.173, No.1 (1998) 10-16.

Rana M.S., Anchetya J., Rayo P., Maity S.K., 'Effect of alumina preparation on hydrodemetallization and hydrodesulfurization of Maya crude', *Catal. Today,* **98** (2004) 151.

Rangwala H.A., Dalla Lana I.G., Otto F.D., Yeniova H. and Al-Nuaimi K., 'Influence of catalyst properties and operating conditions on hydrodenitrogenation of quinoline', *Energy and Fuels*, Vol.**4**, No.5, (1990)599-604.

Rankel L. A., 'Hydroprocessing of Heavy Oil over CoMo/Carbon Supported Catalysts', *Energy & Fuels*, 7(1993)937-942.

Ratnasamy P., Knözinger H., 'Infrared and optical spectroscopic study of Co-Mo-Al$_2$O$_3$ catalysts', *J. Catal.*, **54** (1978) 155-165.

Ratnasamy P., Ramaswamy A.V., Sivasanker S., 'Basic molecules as probes for the study of mo-alumina catalysts', *J. Catal.,* **61** (1980) 519-522.

Rives A., Payen E., Hubaut R., Vazquez P., Pizzio L., Caceres C. and Blanco M., 'Silica and alumina impregnated with dimethylformamide solutions of molybdophosphoric or tungstophosphoric acids for hydrotreatment reactions', *Catal. Lett.*, **71**(2001)193-201.

Rob van Veen J. A., '*Hydrocracking and Catalytic Dewaxing'***,** Handbook of Heterogeneous Catalysis, Volume 6, Second Edition, Wiley VCH, 2778-2808.

Russo P.A., Manuela M., Carrott L.R., Carrot P.J.M., 'Effect of hydrothermal treatment on the structure, stability and acidity of Al containing MCM-41 and MCM-48 synthesised at room temperature', *Colloids and Surfaces A: Physicochem. Eng. Aspects,* **310** (2007) 9-19.

Sakanishi K., Nagamatsu T., Mochida I., Whitehurst D.D., 'Hydrodesulfurization kinetics and mechanism of 4,6-dimethyldibenzothiophene over NiMo catalyst supported on carbon', *Journal of Mol. Catal. A: Chemical* **155** (2000) 101–109

Santes V., Herbert J., Cortez M.T., Zarate R., Diaz L., Swamy P.N., Aouine M., Vrinat M., 'Catalytic hydrotreating of heavy gasoil FCC feed on alumina-titania supported NiMo catalysts', *Applied Catalysis A: General*, **281** (2005) 121-128.

Schlatter J.C., Oyama S.T., Metcalfe J.E. III and Lambert J.M. Jr., 'Catalytic behavior of selected transition metal carbides, nitrides, and borides in the hydrodenitrogenation of quinoline', *Ind. Eng. Chem. Res.*, Vol.27, No.9, (1988) 1648-1653.

Segawa K., Hall W.K., 'Catalysis and surface chemistry: III. The adsorption of pyridine on molybdena-alumina catalysts', *J Catal.*, **76** (1982) 133-143.

Speight J., Chemistry and Technology of Petroleum, Fourth Edition, CRC Press.

P.W. Tamm, H.F. Harnsberger, A.G. Bridge, *Ind. Eng. Chem. Process Des. Dev.*, **20** (1981) 262.

Ware R.A, Wei J., 'Catalytic Hydrodemetallation of Nickel Porphyrins', *J.Catal.*, **93** (1985) 100-121.

Wei J., '*Hydrodemetallation'*, Handbook of Heterogeneous Catalysis , Volume 6, Second Edition, Wiley VCH, 2718-2728.

Weitkamp J. , '*Alkylation of Isobutane with Light Alkenes on Solid Catalysts'* , Handbook of Heterogeneous Catalysis , Volume 6, Second Edition, Wiley VCH, 2830-2853.

Williams C.C., Ekerdt J.G., Jehng J.M., Hardcastle F.D., Turek A.M., Wachs I.E., 'A Raman and ultraviolet diffuse reflectance spectroscopic investigation of silica-supported molybdenum oxide', *J. Phys. Chem.,* **95** (1991) 8781-8791.

Zhao D., Huo Q., Feng J., Kim J., Han Y. and Stucky G. D., *Chem. Mater.,* 11 (1999) 2668.

Zhao D., Huo Q., Feng J, Chmelka B F and Stucky G D , *J. Am. Chem. Soc.,* 120 (1998) 6024**; Zhao D, Huo Q, Feng J, Huo Q, Melosh N, Fredrickson G H, Chmelka B F and Stucky G D,** *Science,* 279 (1998) 548.